

Supplementary Materials for

Metabolic asymmetry and the global diversity of marine predators

John M. Grady*, Brian S. Maitner, Ara S. Winter, Kristin Kaschner, Derek P. Tittensor,
Sydne Record, Felisa A. Smith, Adam M. Wilson, Anthony I. Dell, Phoebe L. Zarnetske,
Helen J. Wearing, Brian Alfaro, James H. Brown

*Corresponding author. Email: jgradym@gmail.com

Published 25 January 2019, *Science* **363**, eaat4220 (2019)
DOI: [10.1126/science.aat4220](https://doi.org/10.1126/science.aat4220)

This PDF file includes:

Materials and Methods

Table S1

Figs. S1 to S10

Caption for data S1

References

Other supplementary material for this manuscript includes:

Data S1 (Excel format)

Materials and Methods

Species distributions and spatial analysis

Richness and phylogenetic diversity were calculated from individual species distribution maps. Marine bird distributions were acquired from BirdLife International (51) and mammal, fish, and reptile distributions from the IUCN (52). Missing or erroneous species distributions were taken from Aquamaps (53) using a 0.5 probability of occurrence criterion. Aquamaps produces standardized range maps for marine species using a niche modelling approach and observation harvest data from OBIS (www.iobis.org). Distribution data were gridded and aggregated for analysis; occurrence was considered as the nonzero overlap of polygon ranges with gridded cells. Cell values in Fig. 1B are projected from Fig 1A onto a $1.0^\circ \times 1.0^\circ$ WGS84 coordinate reference system; all other displayed and analyzed spatial data use a Behrmann equal area WGS84 grid cells of 110 km x 110 km grid cells. Analyses were performed in *R* v. 3.5.1 (ref (54). Phylogenetic data was taken from refs. (55-59) and Faith's phylogenetic diversity – the minimum sum of branch lengths for co-occurring species (7) – was calculated for each taxon using the function *sp* in the *picante* (60) package for *R*. Phylogenetic diversity for mammals and birds with multiple trees were iterated 100 times and averaged. All regression fits and scatterplots exclude spatial cells over 50% land or cells greater than 10% mean annual ice cover, which limits occurrence in air-breathing endotherms and accurate measurement of NPP (see below).

For model predictions, we accounted for spatial autocorrelation in the gridded datasets using two spatial Hierarchical Bayesian models (61) ('bym' and 'besagproper'), which employ integrated nest Laplace approximation methods implemented in *R-INLA* (62, 63) (Table S1).

For Figs. 1 and 2, predators are comprised of speciose, large-bodied clades of that occur primarily in shallow waters (< 200 m depth). Ectothermic teleosts include groupers (Epinephalinae), barracuda (*Sphyraena*), jacks (*Caranx* and *Seriola* in Carangidae), ectothermic scombrids (Scomberomorini & Sardini in Scombridae); other ectotherms include sea snakes (marine members of Hydrophiinae) and sharks (Selachimorpha), excluding mesothermic species. Mesothermic teleosts include tuna (Thunini) and *Gasterochisma melampus* in Scombridae, billfish (Istiophoridae & Xiphiidae); mesothermic sharks comprise mackerel sharks (Lamnidae) and thresher sharks (Alopiidae). Endotherms include all oceanic cetaceans and pinnipeds, 2 species of marine otters (*Lontra felina* and *Enhydra lutris*), and all swimming, marine birds with pursuit diving strategy: penguins (Spheniscidae), auks (Alcidae), and marine species of cormorants (Phalacrocoracidae), grebes (Podicipedidae), and loons (Gaviidae). Bird species were classified as marine if species ranges extended into the ocean or had coastal ranges and were characterized in Handbooks of Birds of the World Alive (64) as predominantly or seasonally marine foragers.

Locomotory and metabolic rates

Data on locomotory and metabolic rates were compiled from the literature including speeds for pinnipeds (65-70), penguins (71-74), and dolphins (75, 76). Fish speeds have been measured in various way, including whole body movement that vary with the duration of measurement and acclimation, as well as calculation from muscle contraction rates (77). To ensure standardized data, we use rates from species compiled by Wardle (78), where muscle contraction time m and body length L was used to calculate burst speeds S of fish in Fig. 3b, where $S = 0.7L/2m$. Fish data for Fig. 3b includes one species of tuna, but at small individual sizes (< 36 cm length) where tuna are effectively ectothermic (79). See also Fig. S4.

Mammal Consumption

Annual mammal consumption and abundance was analyzed using 110 km x 110 km grid cells. Mammal total consumption and abundance data were previously estimated from a compilation of published abundance records for all cetacean and pinniped species and metabolic scaling of consumption with body size (27, 28), building on prior assessments . Spatially-explicit estimates of species-specific consumption rates of prey (tonnes wet mass spatial cell⁻¹ yr⁻¹) and

densities were produced by linking totals to predicted relative species occurrence in a GIS framework (27). These predictions of species-specific relative environmental suitability were derived using a niche modeling approach and published information about evolutionary origin and habitat preference of species with respect to sea surface temperature, depth and distance from the ice edge and, for a few otariid species, distance to land (28). Niche preferences for distance to land (e.g., coastal vs oceanic), distance from ice, water temperature, and evolutionary origin were gathered from the literature and used to construct range maps for each marine mammal species and estimate species density across space. This largely captures whether a species is tropical, temperate and/or polar, coastal and/or oceanic, requires ice or land to breed, and is restricted to an ocean basin. Niche modeling of abundance distributions did not include productivity as a predictor variable, ensuring independence from model tests.

Small toothed whales considered here (i.e., odontocetes excluding Ziphiidae, Physeteridae, Kogiidae, and all freshwater species) feed at a similar trophic level and generally close enough to surfaces for sea surface temperature to be a relevant predictor of ambient water temperature during foraging (29). Total abundance or consumption rates of pinnipeds or odontocetes with < 10 individuals per spatial cell were excluded.

Baseline Abundance & Diversity in Marine Mammals

Some marine mammal species were subject to intensive harvesting over the past two centuries. However, several factors minimize bias in our estimation of the distribution, abundance and consumption of predatory marine mammals. First, patterns of diversity are unlikely to be greatly impacted due to the rarity of historical marine mammal extinction (only 3 of ~135 species, ref. (80)), as well as the large home ranges of many marine mammal species (81). Second, with respect to marine mammal abundance and consumption, industrial harvesting primarily focused on baleen whales (82) which, as predominantly planktonic feeders, were not considered in estimation of $C_{TotEndo}$. In addition, a recent synthesis indicates that many marine mammal populations have experienced substantial recoveries, ~60 – 90% recovery for pinnipeds, delphinids and porpoises (26). Finally, our results are conservative and robust to declines in marine mammal consumption and abundance. Global declines in consumption will primarily affect the intercept in Fig. 5B ($\ln(b_1)$ in Eq. 6), not the slope E_f , unless consumption rates approach carrying capacity. For instance, a 10fold decline in all mammal consumption has no

effect to 3 decimal points of E_f . Assuming ~1% of NPP converts to prey production (consistent with (30)), a 10fold increase in global mammal consumption generates a slightly higher estimate of $E_f = 1.27$ (CI: 1.26 – 1.28) that falls within the theoretically predicted range.

Modeling Encounter Rates & Capture Efficiency

Encounter rates are frequently modeled as a function of predator and prey relative or combined velocities V_c , calculated as the root mean square of predator and prey velocities: $V_c = \sqrt{V_{Pred}^2 + V_{Prey}^2}$ (ref. (5)). Because the dot product of two vectors is a scalar, this can be rewritten in terms of speed S . For most marine predators, predators are significantly larger than prey (83). Burst speed is a power function of body length L , where the slope has been found to be 0.5, or as high as 1 (refs. (21, 84); thus, burst speed is typically greater in predators. Because speeds are squared when calculating V_c , the predator speed dominates the mean square term. As an illustration, consider a hypothetical 1 m ectothermic predator with a burst speed of 2 m/s pursuing a 0.1 m fish. Taking the more conservative scaling exponent of 0.5, S_{Pred} is $2 = aL^{0.5}$ and $S_{Prey} = aL^{0.5}$, where a is a normalization constant. The root mean square of predator and prey speeds is 2.098 m/s, i.e., ~predator speed. Thus, for most species, V_c can be generally approximated as S_{Pred} , simplifying calculations. For specific taxa, explicit parameterization of body mass effects on foraging rates can be included, following refs (5, 21).

Model

Eq. 6 can be derived from Eq. 4 and 5 by noting that, after substitution of Eq. 4, Eq. 5 becomes: $C_{TotEndo} = P_{Prey}/(1+b/b_0e^{E_f/kT})$, where b_0 is a normalization constant. This can be rewritten as $P_{Prey}/C_{TotEndo} = 1 + (b/b_0)e^{-E_f/kT}$, then $\ln(P_{Prey}/C_{TotEndo} - 1) = -(1/kT)E_f + \ln(b_1)$, where $b_1 = b/b_0$. It is useful to write this in a slope-intercept form as $\text{logit}(C_{TotEndo}/P_{Prey}) = E_f(1/kT) - \ln(b_1)$, where the slope is E_f and the response variable is a measure of relative consumption, i.e., the proportion of prey production consumed by marine endotherms, bounded by 0 and 1 at equilibrium.

We use pinniped and small odontocete consumption as a proxy for endotherm predatory consumption in the ocean, $C_{TotEndo}$. We model $C_{TotEndo}$ as a Hill function where endotherm consumption rate decelerates as it approaches the limit of total available prey production (Eq. 5, 6). Estimating prey production from NPP is complex, but below the asymptote, the slope of

$\text{logit}(NPP/C_{TotEndo})$ vs $1/kT$ yields a conservative approximation of $\text{logit}(P_{Prey}/C_{TotEndo})$ vs $1/kT$. To illustrate this, we calculate prey production from NPP assuming a simple trophic structure, consistent with Pauly & Christensen (PC) (30). Here $P_{Prey_PC} = 9 * (NPP) (TE)^{TL-1}$, where 9 is a conversion unit of algae carbon mass to fish wet mass, TE is the trophic transfer efficiency equaling 0.1, and TL is trophic level of the prey. Gut analysis indicates that endotherms generally feed on planktivorous fish (29) and TL of 3 is assigned. Using P_{Prey_PC} yields a slope of 1.08 for the CbPM model of NPP, substitution of NPP returns a slope of 1.05 (Table S1). As the C_{Tot}/P_{Prey} ratio declines, the slope converges on the slope for C_{Tot}/NPP .

Our model implies a zero sum game of prey consumption between endotherms and ectotherms. As a result, competition and individual foraging success are linked: declines in endotherms promotes gains in ectotherms. Because of their higher metabolic needs, endotherms may be excluded from some low-resource environments or niches independent of competition from ectotherms, such as the deep sea. In marine systems, the most unproductive portions available to air-breathing endotherms are the open-ocean subtropics (12, 14). Even here, however, endothermic dolphins persist by efficient cooperative foraging, tracking of transient fish schools, and pursuit of abundant mesopelagic fish at depth (85).

Assumptions and Uncertainties

The global diversity patterns and theoretical model presented here should be interpreted in context. We focus on interspecific variation in metabolism and its consequences on foraging and distribution globally. Thus, across species and over broad thermal gradients metabolic rates of endotherms and ectotherms are predicted to follow Eq. 1. Within a species, rates will depart from Eq. 1 when species are exposed to atypical or non-preferred environmental temperatures, e.g. near critical thermal minima/maxima or above thermal optima for ectotherms (see (86)). For ectotherm-ectotherm interactions, deviation in thermal performance curves or warming/cooling rates can also generate metabolic and performance asymmetries that are relevant to foraging and competition (5); however, these will not lead to systematic interspecific shifts across latitudes or global thermal gradients. To incorporate temperature dependence within a species, as well as variation in body size, more complex permutations of Eq. 1 can be used (5), and handling time can be included using a Type II functional response (87). Systematic shifts in consumption with temperature from Eq. 6 are predicted in broad, active foraging guilds of endotherms or

ectotherms. We focus on competitive shifts between thermoregulatory guilds; within endotherms, demographic shifts with temperature will be modulated by competition from other endothermic species that occupy warmer or cooler regions of a competitor's fundamental niche (e.g., Fig. S9).

A distinctive feature of our foraging model is its focus on the metabolic drivers of capture efficiency C_e . It is important to note that metabolic asymmetries are only relevant to C_e where prey is difficult to capture, e.g. in most active capture scenarios. Where $S_{Pred} \gg S_{Prey}$, as in the case of foraging for slow, sessile or planktonic prey, the role of thermally-mediated asymmetries driving capture efficiency declines to zero ($C_e \propto T^0$ and $E_I = 0$).

Although mammal abundances represent empirical syntheses, spatial distributions of abundance were calculated from niche modeling of abiotic environmental preferences described in ref. (27). Finer grained abundance patterns likely also reflect locations and densities of prey patches within a species range; thus, intraspecific variation in abundance within a species' range may be underestimated. This should have limited influence, however, on estimates of global, interspecific consumption across latitudes.

Environmental variables

Bathymetry data is from (88, 89). We used a decadal average of monthly ice cover (90, 91) and sea surface temperature (91, 92) from years 2006 – 2015. Marine spatial cells were considered ice-covered if they averaged 10% or greater mean ice cover over this period. A decadal average of Net Primary Production (NPP) from the same period was generated by averaging monthly data from the Ocean Productivity website (93, 94).

NPP was only used for analysis in ice free cells, as NPP below ice can be substantial and is not easily measured (95). We assessed theoretical predictions using three different models of NPP (Fig S7: Vertically Generated Production Model (VGPM) (93), the Eppley-VGPM (Eppley) (96, 97), and the Carbon based Production Model (CbPM) (98). The Eppley and VGPM use spectral data to estimate chlorophyll densities and the Eppley model differs primarily by modeling higher growth response phytoplankton in warm water. Empirical growth analyses of phytoplankton generally support the thermal parameters of the Eppley (99, 100), and *in situ* tests found the Eppley model to better predict NPP than the VGPM (101). The more recent CbPM model is qualitatively similar to the Eppley model but utilizes light backscattering to link algae

chlorophyll to biomass and better accounts for seasonal variation in production (98). Irrespective of the NPP model used, all slopes of consumption vs sea surface temperature fall within the predicted range of $0.65 \leq E_f \leq 1.3$ (Table S1). Plots of environmental variables can be found in Fig. S7.

Linking NPP to Prey Production

Net primary production underpins virtually all biological productivity at sea, including production rates of marine mammal prey. The relationship between NPP and higher trophic production reflects several factors, including producer size, the number of trophic levels, zooplankton growth efficiency and the strength of zooplankton-phytoplankton coupling (i.e., the fraction of primary production that is consumed by zooplankton). In general, productive, seasonal seas are characterized by larger phytoplankton and fewer trophic levels, but weaker zooplankton-phytoplankton trophic coupling (102, 103). Small fish that comprise large marine mammal diets are typically planktivorous (29), feeding on larger mesozooplankton (MZ) where MZ are (0.2 – 200 mm). Although mesozooplankton production (Mzp) modeling has received less attention than NPP, recent efforts offer spatially-explicit estimates. Stock *et al* used a geochemical model ocean model with global sampling of MZ biomass to estimate continuous global MZ abundance and production (14, 104). They observed the relationship between NPP and planktivorous fish production to largely reflect three factors: mesozooplankton trophic level above phytoplankton (*MTL*), zooplankton growth efficiency (*ZGE*), and the strength of zooplankton-phytoplankton trophic coupling (*ZPC*), i.e., the fraction of phytoplankton consumed by zooplankton, where $Mzp \cong NPP * ZPC * ZGE^{MTL}$.

We use Mzp values from Stock *et al* (14) in lieu of NPP to test model predictions. Results are quantitatively similar and consistent with theory, where $E_f = 0.947$ (CI: 0.937 – 0.957, $r^2 = 0.56$; Fig S8). Discrepancies between Mzp and NPP are largely found in subtropical gyres, where Mzp is comparatively lower. Plant and animal production has been traditionally considered to be very low in the subtropics (105) but more recent research suggests this may be underestimated (85, 106) and the issue is an ongoing area of study.

Table S1. A summary of models and parameter values. Slopes for regression fits are shown with 95% confidence/credible intervals for linear model (LM) and Bayesian models (BYM and BP), in parentheses. LM fits are accompanied by r^2 values. BYM refers to the ‘bym’ and BP to the ‘besagproper’ methods that partition spatial autocorrelation from main effects (63). Slopes are derived from regression against sea surface temperature °C (SST°C) or inverse sea surface temperature ($1/kT$) where k is a Boltzmann factor (8.617×10^{-5} eV), and T is sea surface temperature in Kelvins. Slopes for consumption vs. $1/kT$ represent estimates of E_f . Rel_Richness is the ratio of endotherm to ectothermic richness depicted Fig. 1; tests include a variant that excludes planktivorous baleen whales (mysticetes). NPP refers to Net Primary Production (tons wet mass $\text{yr}^{-1} \text{cell}^{-1}$), as estimated from three models (CbPM, Eppley-VGPM, VGPM). C_{TotMam} is consumption by pinnipeds and small toothed whales (i.e., odontocetes excluding sperm and beaked whales). MZP is mesozooplankton production in tons per year per cell area km^{-2} , C_{TotPin} is total pinniped consumption. Coastal refers to whether a cell is coastal (not exclusively marine or < 200 m depth) or oceanic, Dist is the distance (km) of a spatial cell center from land, Chlor is the mean chlorophyll concentration (mg C m^{-2}) of a cell, depth is the mean depth of a cell in meters, P_{Prey_PC} refers to the conversion of NPP to prey production following Pauly and Christensen (30) (see *Methods*). Abun is abundance.

Supplementary Table

Table S1 | Model Tests

Model	Slope	Adj. r^2
Richness		
LM $\ln(\text{Rel_Richness}) \sim \text{SST}^\circ\text{C}$	-0.108 (-0.110 – -0.107)	0.43
LM $\ln(\text{Rel_Richness}) \sim \text{SST}^\circ\text{C}$ (no mysticetes)	-0.104 (-0.105 – -0.102)	0.42
LM $\ln(\text{Rel_Richness}) \sim \text{SST}^\circ\text{C} + \text{Coastal}$	-0.109 (-0.110 – -0.108)	0.62
BP $\ln(\text{Rel_Richness}) \sim \text{SST}^\circ\text{C} + \text{Coastal}$	-0.0887 (-0.0912 – -0.0703)	
BYM $\ln(\text{Rel_Richness}) \sim \text{SST}^\circ\text{C} + \text{Coastal}$	-0.0578 (-0.0621 – -0.0536)	
Total Consumption		
LM $\ln(C_{\text{TotMam}}) \sim \text{SST}^\circ\text{C}$	-0.105 (-0.106 – -0.104)	0.71
LM $\ln(C_{\text{TotMam}}) \sim \ln(\text{NPP}_{\text{CbPM}})$	-1.09 (-1.11 – -1.06)	0.26

LM $\ln(C_{\text{TotMam}}) \sim \ln(\text{NPP}_{\text{Eppley}})$	-0.487 (-0.507 – -0.468)	0.082
LM $\ln(C_{\text{TotMam}}) \sim \ln(\text{NPP}_{\text{VGPM}})$	0.349 (0.328 – 0.370)	0.038
Relative Consumption		
<i>NPP Tests</i>		
LM logit($C_{\text{TotMam}}/\text{NPP} \sim 1/kT$)	1.05 (1.04 – 1.05)	0.80
LM logit($C_{\text{TotMam}}/\text{NPP}_{\text{Eppley}} \sim 1/kT$)	1.00 (0.995 – 1.01)	0.74
LM logit($C_{\text{TotMam}}/\text{NPP}_{\text{VGPM}} \sim 1/kT$)	0.700 (0.692 – 0.707)	0.55
BYM logit($C_{\text{TotMam}}/\text{NPP} \sim 1/kT$)	0.696 (0.666 – 0.725)	
BP logit($C_{\text{TotMam}}/\text{NPP} \sim 1/kT$)	0.778 (0.732 – 0.823)	
LM logit($C_{\text{TotMam}}/\text{NPP} \sim 1/kT + \text{Dist} + \ln\text{Chlor} + \text{Depth}$)	1.18 (1.17 – 1.18)	0.87
<i>Prey & MZP Tests</i>		
LM logit ($C_{\text{TotMam}}/\text{P}_{\text{Prey_PC}} \sim 1/kT$)	1.08 (1.07 – 1.09)	0.80
LM logit($C_{\text{TotMam}}/\text{MZP} \sim 1/kT$)	0.947 (0.937 – 0.957)	0.56
BP logit($C_{\text{TotMam}}/\text{MZP} \sim 1/kT$)	0.901 (0.854 – 0.949)	
BYM logit($C_{\text{TotMam}}/\text{MZP} \sim 1/kT$)	0.727 (0.686 – 0.768)	
<i>Pinniped Consumption</i>		
LM logit($C_{\text{TotPinn}}/\text{NPP} \sim 1/kT$)	1.72 (1.71 – 1.74)	0.81
BYM logit($C_{\text{TotPin}}/\text{NPP} \sim 1/kT$)	1.67 (1.65 – 1.70)	
BP logit($C_{\text{TotPinn}}/\text{NPP} \sim 1/kT$)	1.48 (1.41 – 1.53)	
LM logit($C_{\text{TotPinn}}/\text{MZP} \sim 1/kT$)	1.55 (1.54 – 1.57)	0.67
BYM logit($C_{\text{TotPinn}}/\text{MZP} \sim 1/kT$)	1.36 (1.33 – 1.39)	
BP logit($C_{\text{TotPinn}}/\text{MZP} \sim 1/kT$)	1.65 (1.58 – 1.71)	
Relative Abundance		
LM $\ln(\text{Abun}_{\text{TotMam}}/\text{NPP}) \sim 1/kT$	0.892 (0.885 – 0.899)	0.69
LM $\ln(\text{Abun}_{\text{TotPinn}}/\text{NPP}) \sim 1/kT$	1.95 (1.93 – 1.96)	0.82

Supplementary Figures

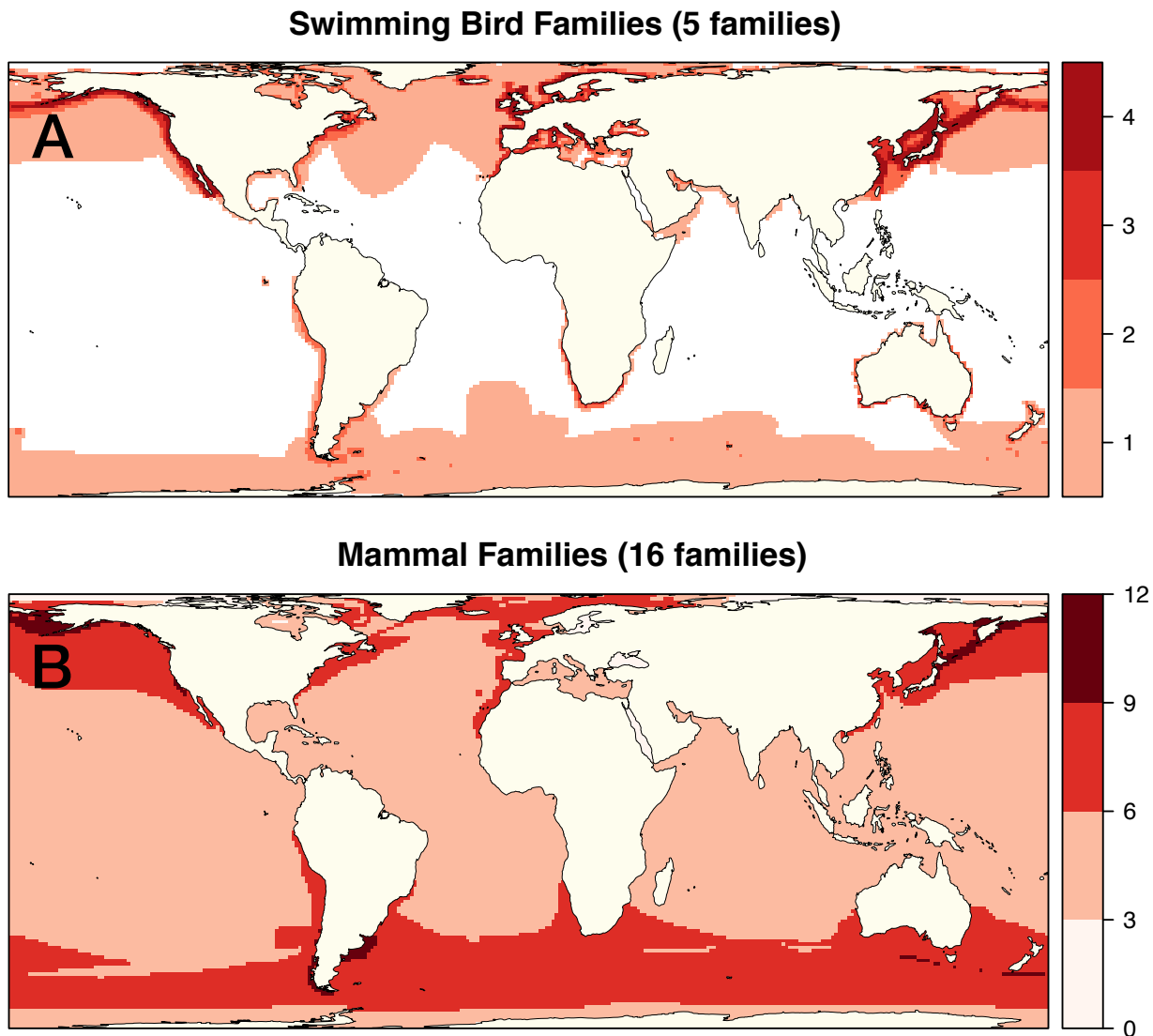
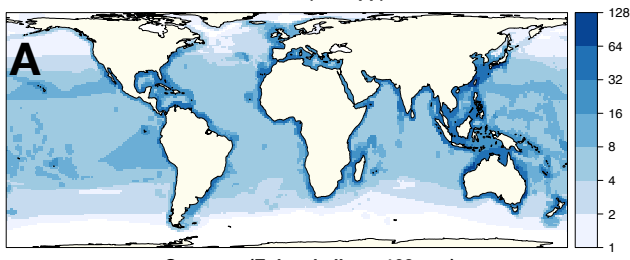


Fig. S1. Number of families of predatory marine mammals and swimming birds. A & B

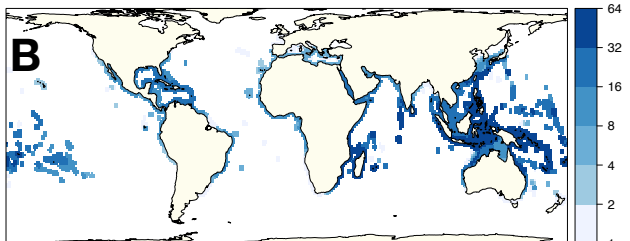
The count of overlapping families of marine swimming birds (penguins, auks, cormorants, grebes, loons) and marine mammals (cetaceans, pinnipeds, otters). White spatial cells indicate areas with no recorded families.

Ectotherm Richness

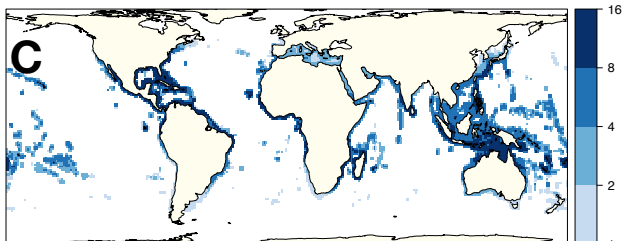
Sharks (467 spp)



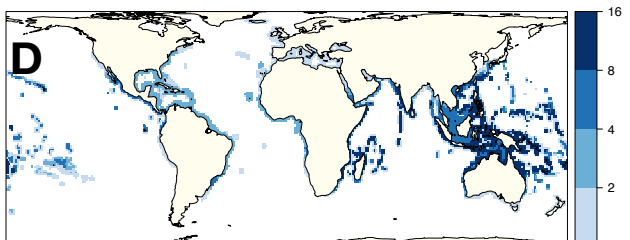
Groupers (Epinephelinae, 162 spp)



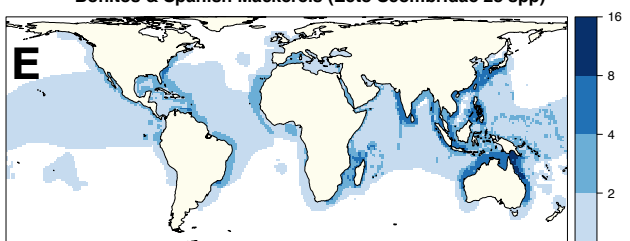
Jacks (Caranx & Seriola, 28 spp)



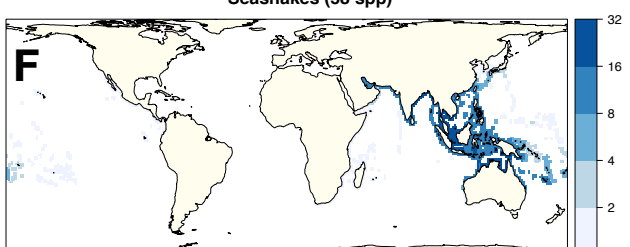
Barracuda (Sphyraena, 25 spp)



Bonitos & Spanish Mackerels (Ecto Scombridae 28 spp)

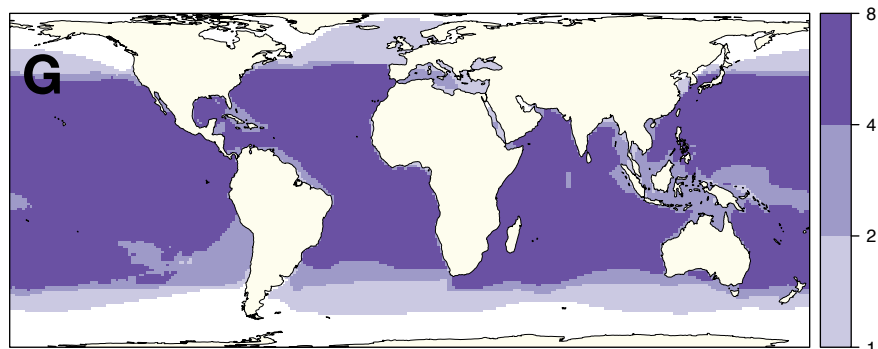


Seasnakes (58 spp)

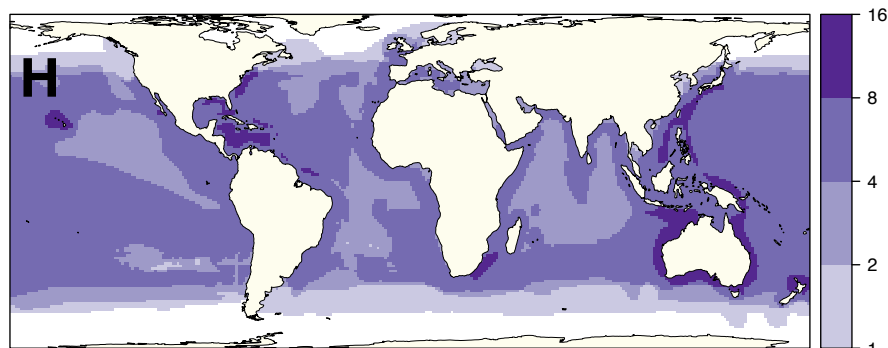


Mesotherm Richness

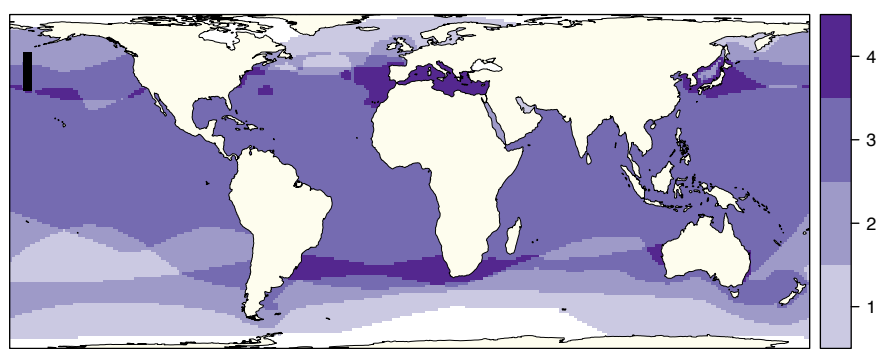
Billfish (Xiphiidae & Istiophoridae 10 spp)



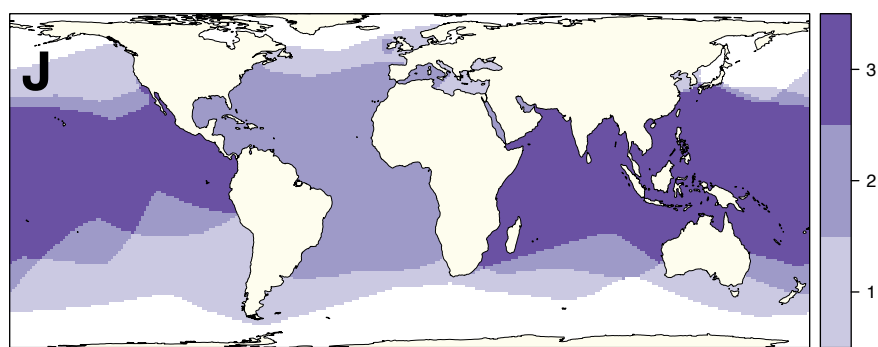
Tuna (Meso Scombridae 16 spp)



Mackerel Sharks (Lamnidae 5 spp)

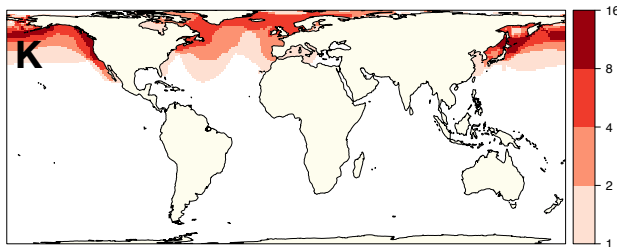


Thresher Sharks (Alopiidae 4 spp)

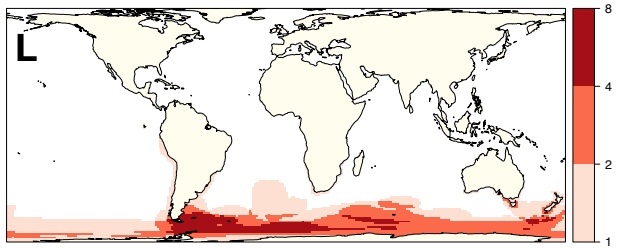


Endotherm Richness

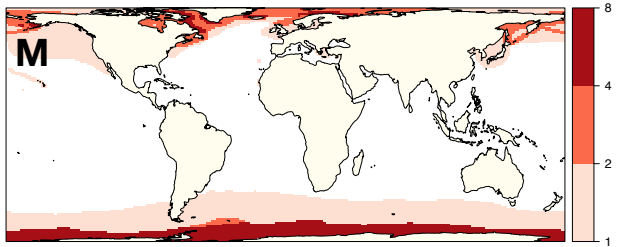
Auks & Puffins (Alcidae, 25 spp)



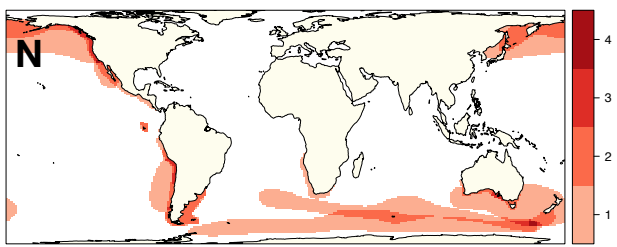
Penguins (Spheniscidae, 18 spp)



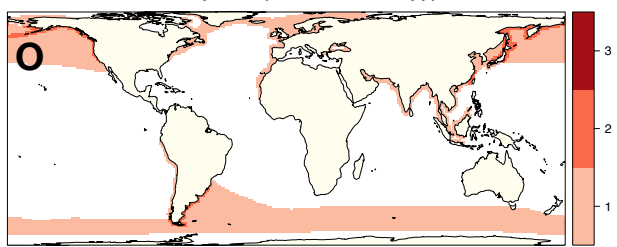
Seals (Phocidae, 15 spp)



Sea Lions & Fur Seals (Otaridae, 15 spp)



Porpoises (Phocoenidae, 7 spp)



Dolphins (Delphinidae, 68 spp)

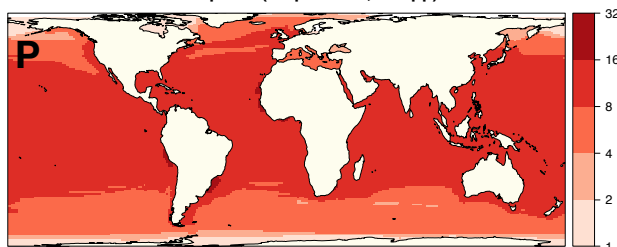


Fig. S2. Species richness for major predatory clades. Thermoregulatory guilds in shallow waters show consistent latitudinal patterns of diversity: **A-F** ectotherms are most diverse in the tropics and subtropics, **G-J** mesotherms are cosmopolitan excluding polar waters, and **K-P** endotherms that are more diverse in colder temperate waters, with the notable exception of dolphins (*Delphinidae*, **P**). All taxon shown are predominantly shallow-water predators. Some low-diversity, endothermic families, such as *Monodontidae* and *Gaviidae*, are not plotted but show similar spatial patterns. White spatial cells indicate areas with no recorded species.

Components of Foraging

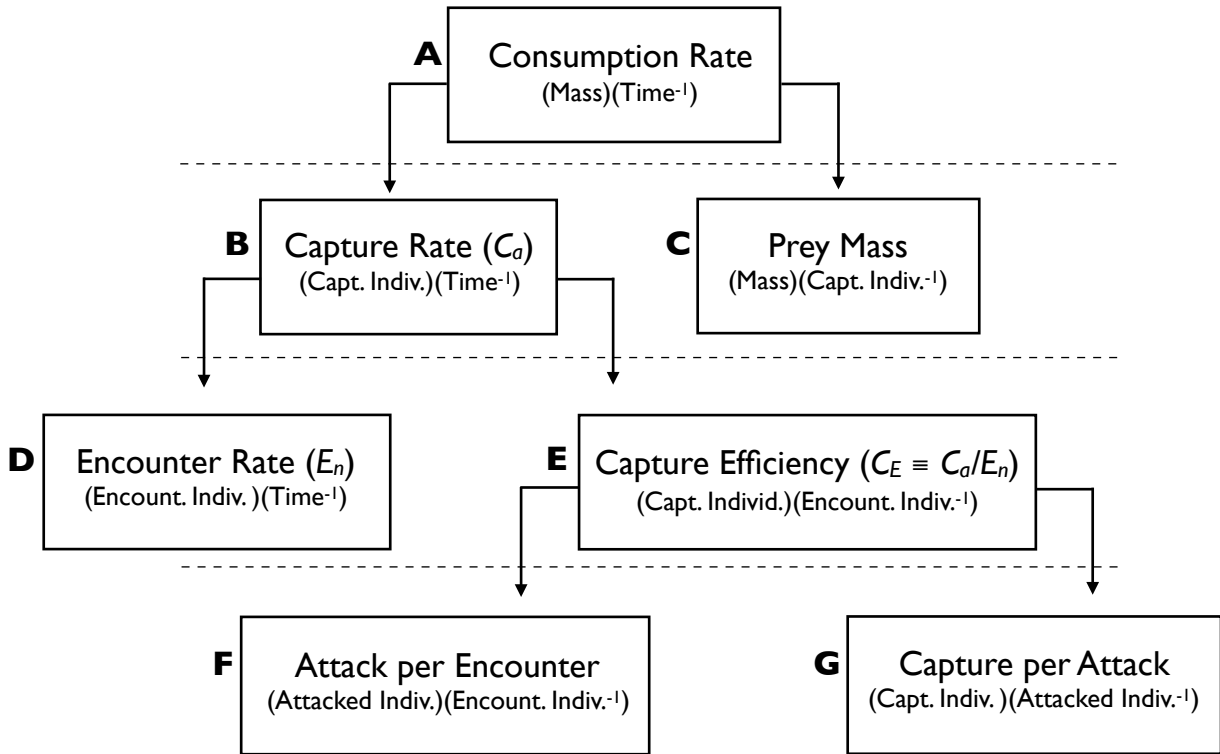


Fig S3. Components of individual foraging. **A-G.** Foraging rates are decomposed into their respective dimensional components, beginning with the individual consumption rate (**A**). Each parameter component box represents the product of succeeding boxes below, as indicated by arrows. The unit dimensions for each parameter is shown in parentheses. Note that for capture efficiency (**E**), the time components of C_a and E_n cancel, yielding a measure of the probability of capture per encounter. For endotherms hunting ectotherms, increased capture efficiency in colder habitats may reflect via higher attack rates per encounter (**F**), and/or higher capture probability per attack (**G**). For very slow or sessile prey, i.e., $S_{Pred} \gg S_{Prey}$, $E_f = 0$ and $C_E \propto T^0$. The associated equations are described in the text and Fig 4. Abbreviations: Capt. is Captured, Encount. is Encountered, Indiv. is the Individual prey item; all other abbreviations are provided in the boxes.

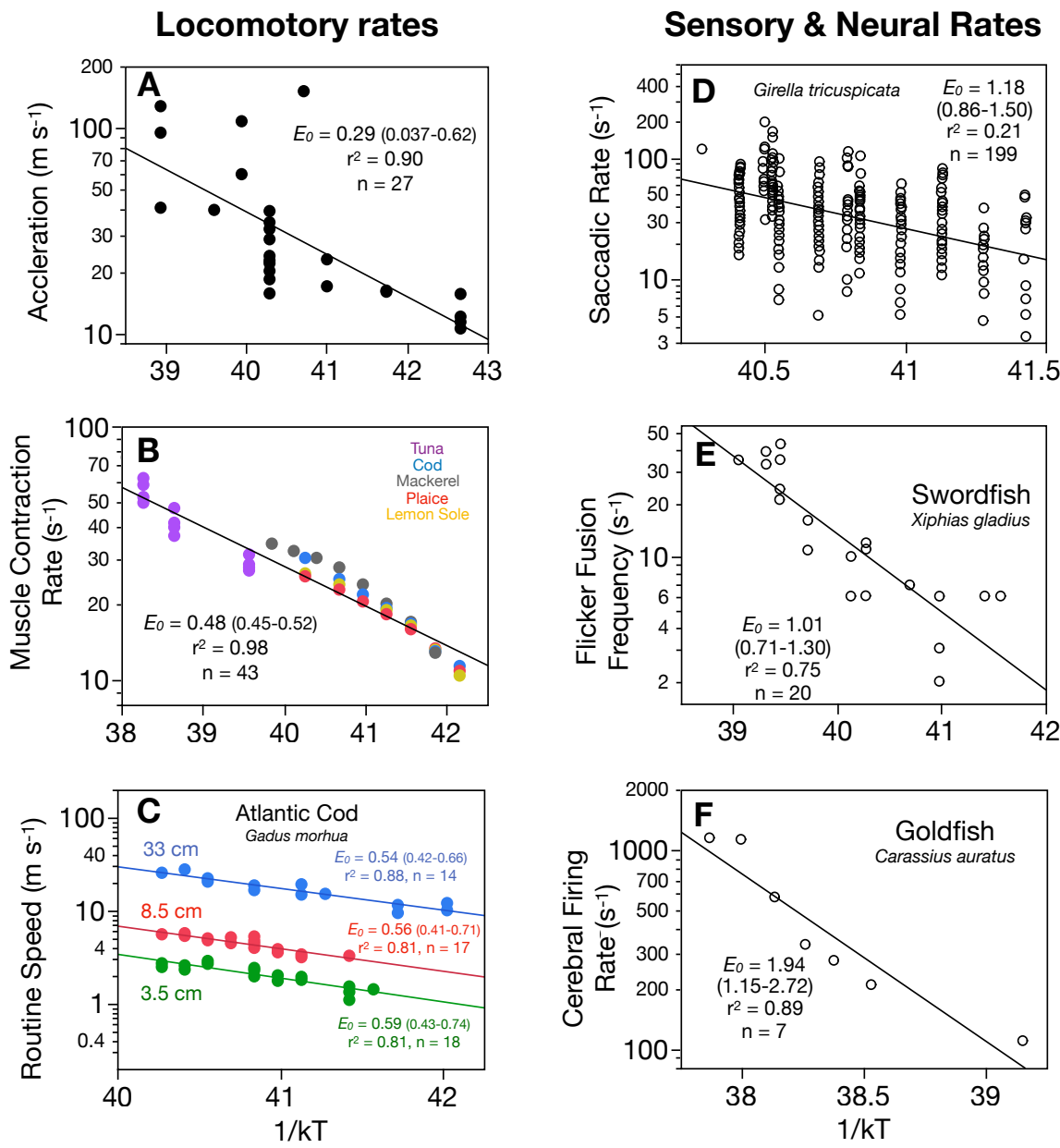
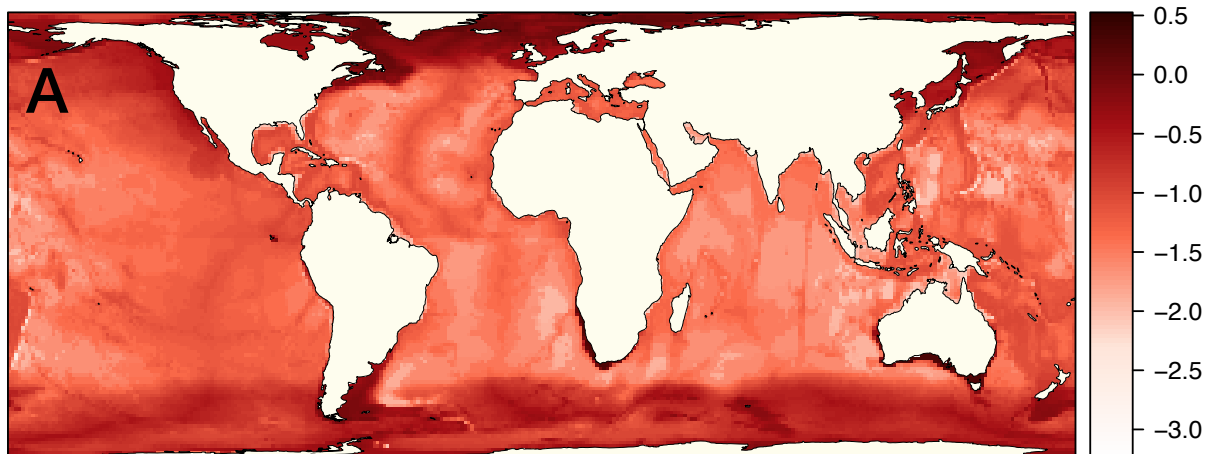
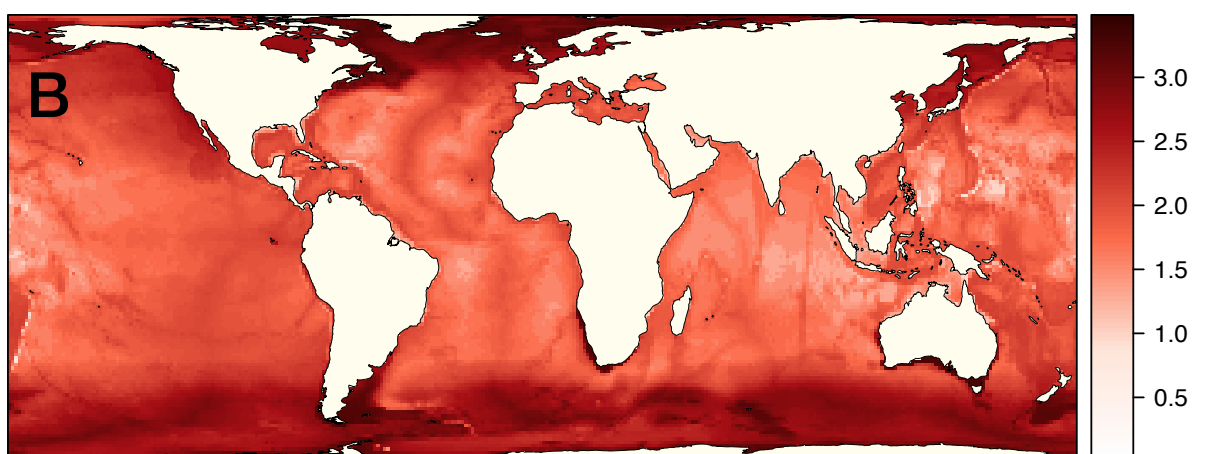


Fig. S4. Thermal dependence of muscular and locomotory A-C and sensory rates D-F. In A, acceleration in fish is approximately size-independent (107), so body size was not standardized; data from (107). For A and B, species identity is included as a predictor variable. For B, all individuals range in length from 35 – 43 cm; data from (78). Data for C is from (108), D is from (109), E is from (25), F from (110). For A – F, 95% confidence intervals are shown in parentheses; $p < 0.01$ for all regressions.

\log_{10} Odontocete & Pinniped Abundance (km^{-2})



\log_{10} Odontocete & Pinniped Consumption ($\text{kg km}^{-2} \text{ yr}^{-1}$)



\log_{10} Consumption/NPP

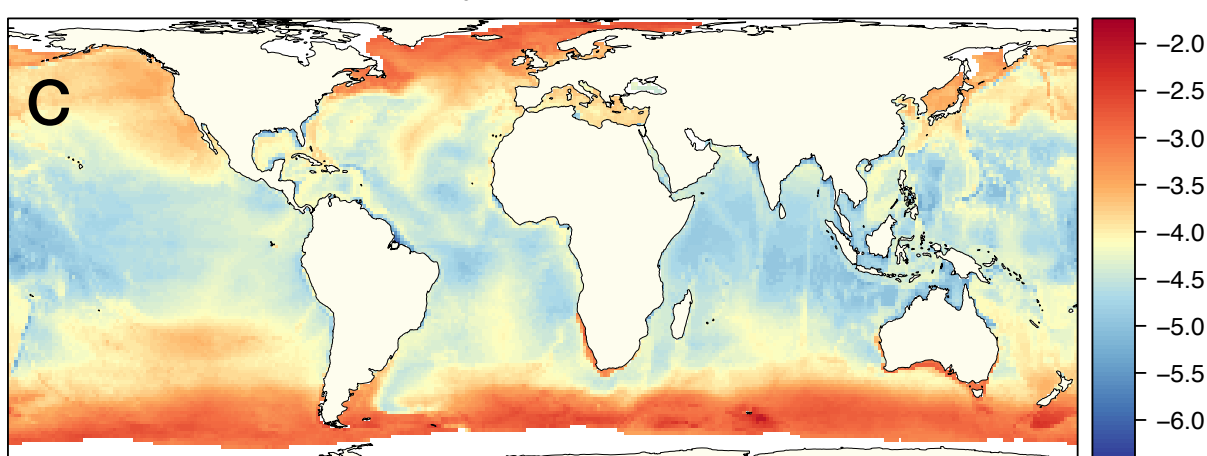


Fig. S5. Global patterns of marine mammal abundance and consumption. **A** Pinniped and small odontocete abundance and **B** consumption increase towards high latitudes with cold surface waters. Data from (28). Note the relatively low abundance and consumption of marine mammals in tropical upwelling zones with high fishery production, such as the Humboldt current along the western coast of South America and the Canary current in northwest Africa. In **C**, the dimensionless ratio of mammal consumption from **B** and net primary production (NPP) is shown, revealing a spatial gradient of relative consumption. Areas under ice or > 50% terrestrial are excluded.

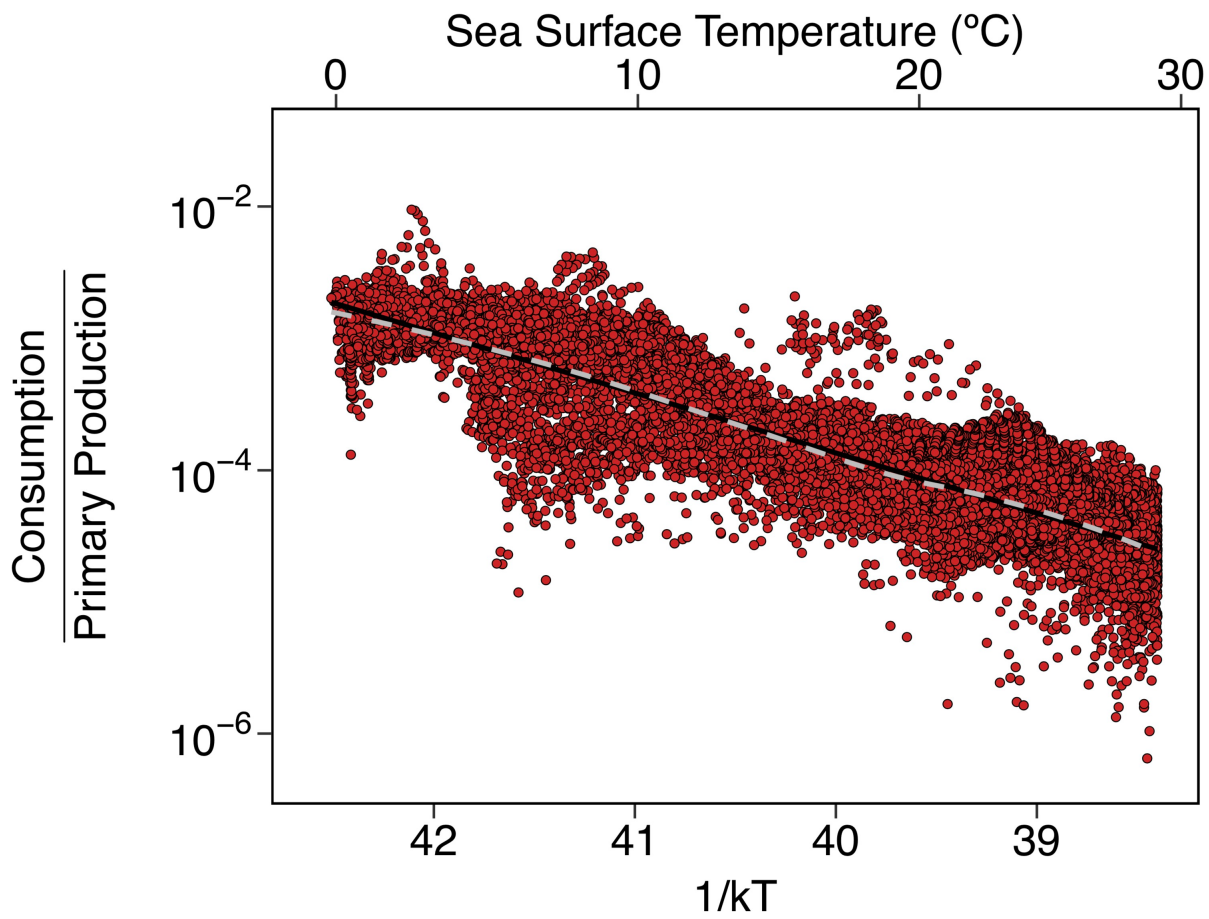
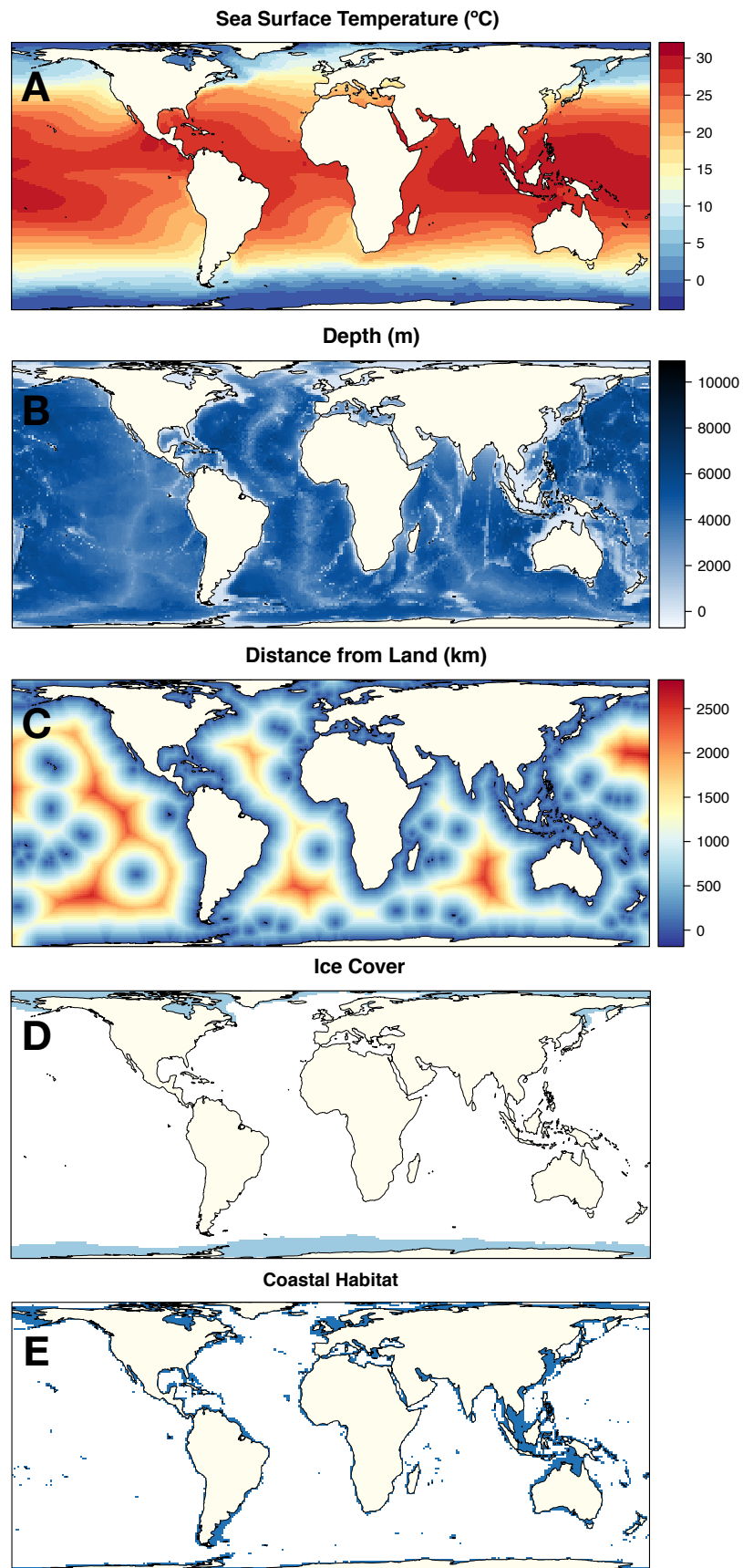


Fig S6. Relative consumption. Fig 5B is replotted, where the linear regression fit (black, solid) is overlaid with a loess fit that shows curvilinearity (gray, dashed; see Fig 5Afor comparison). Despite environmental variation across 26,924 gridded spatial cells, water temperature is a strong linear predictor of relative consumption by marine mammals ($r^2 = 0.80$).



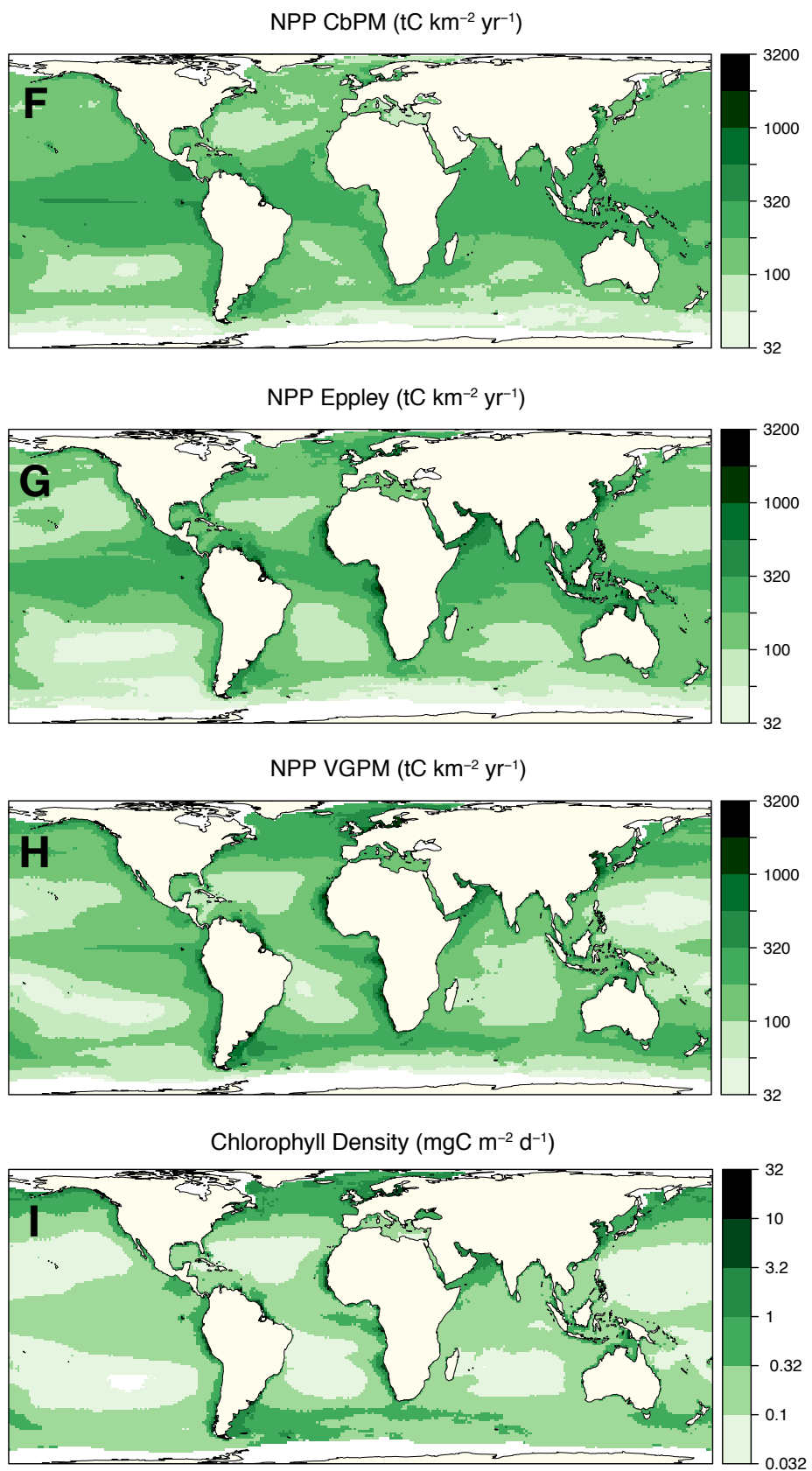


Fig. S7. Environmental variables. For **A**, **D** and **F - H**, data was compiled and averaged across a ten-year period (2006-2015). NPP (CbPM) from **F** was used for all analyses unless otherwise stated; **B**, **C**, and **I** were considered as additional predictor variables (Table S1). Ice cover (**D**) represents spatial cells averaging >10% ice cover across the ten-year period. Coastal habitat (**E**) is defined as cells that overlap land or are < 200 m depth. **G-H** are alternate NPP model outputs evaluated in sensitivity analyses (see Table S1). NPP units are tons carbon per km² per year; values under ice covered cells are excluded. Gridded cells are 110 km x 110 km.

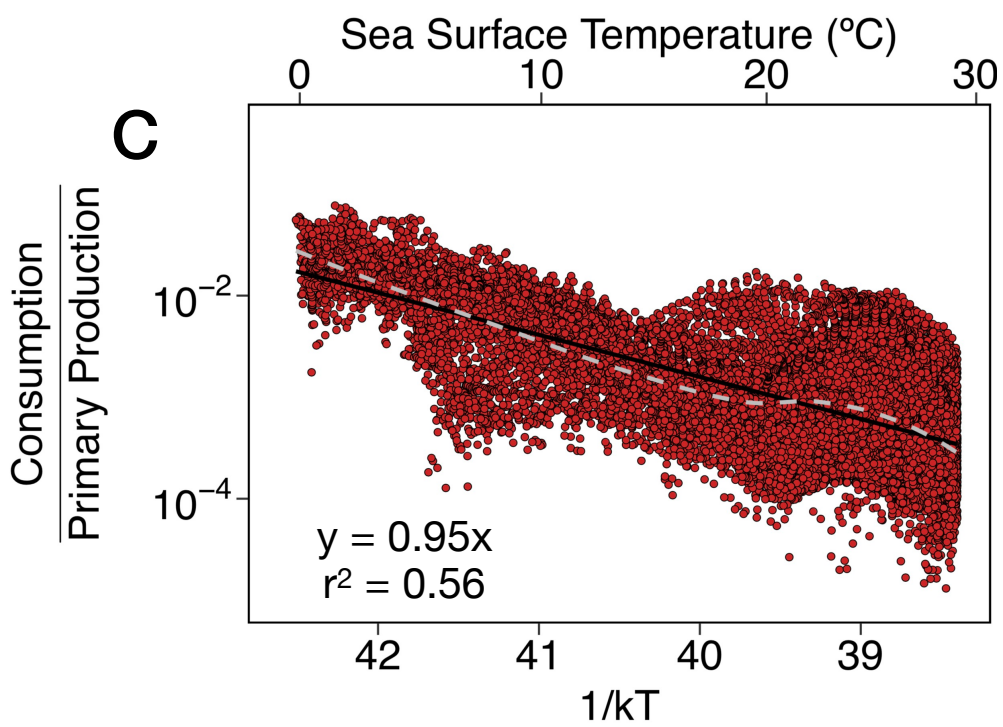
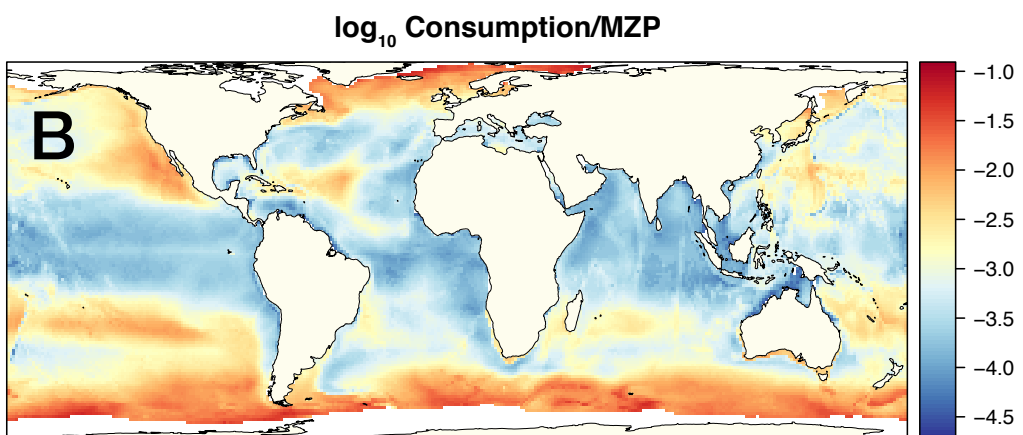
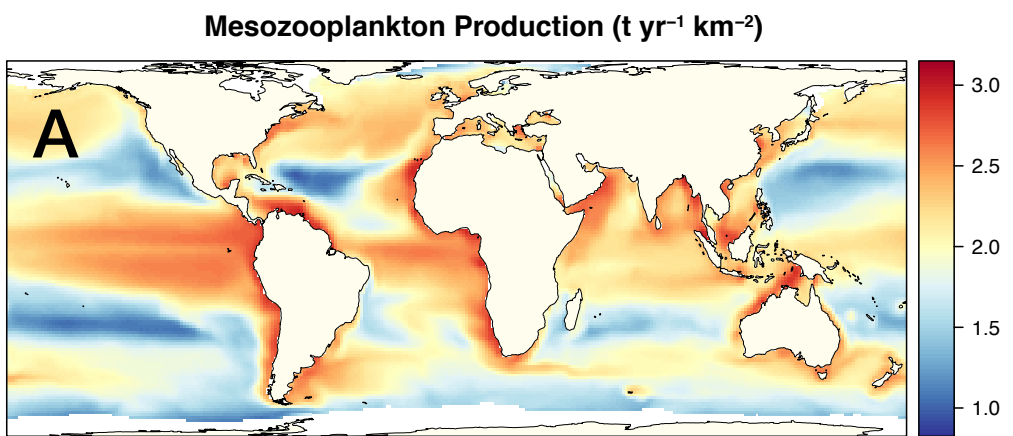


Fig. S8. Marine trophic structure and production. **A** Mesozooplankton production (MZP) in wet mass from Stock *et al* (14), where mesozooplankton are 0.2 – 20 mm length. Values under ice cover are excluded. **B** shows the dimensionless ratio of small odontocete and pinniped consumption per unit mesozooplankton production. **C** In **C**, the ratio observed in **B** is plotted against inverse sea surface temperature ($1/kT$), with Celsius values also shown (top). The dashed gray line is a loess fit. See Fig S5, S6 for comparison. The regression slope is consistent with theoretical predictions (CI: 0.934 – 0.954).

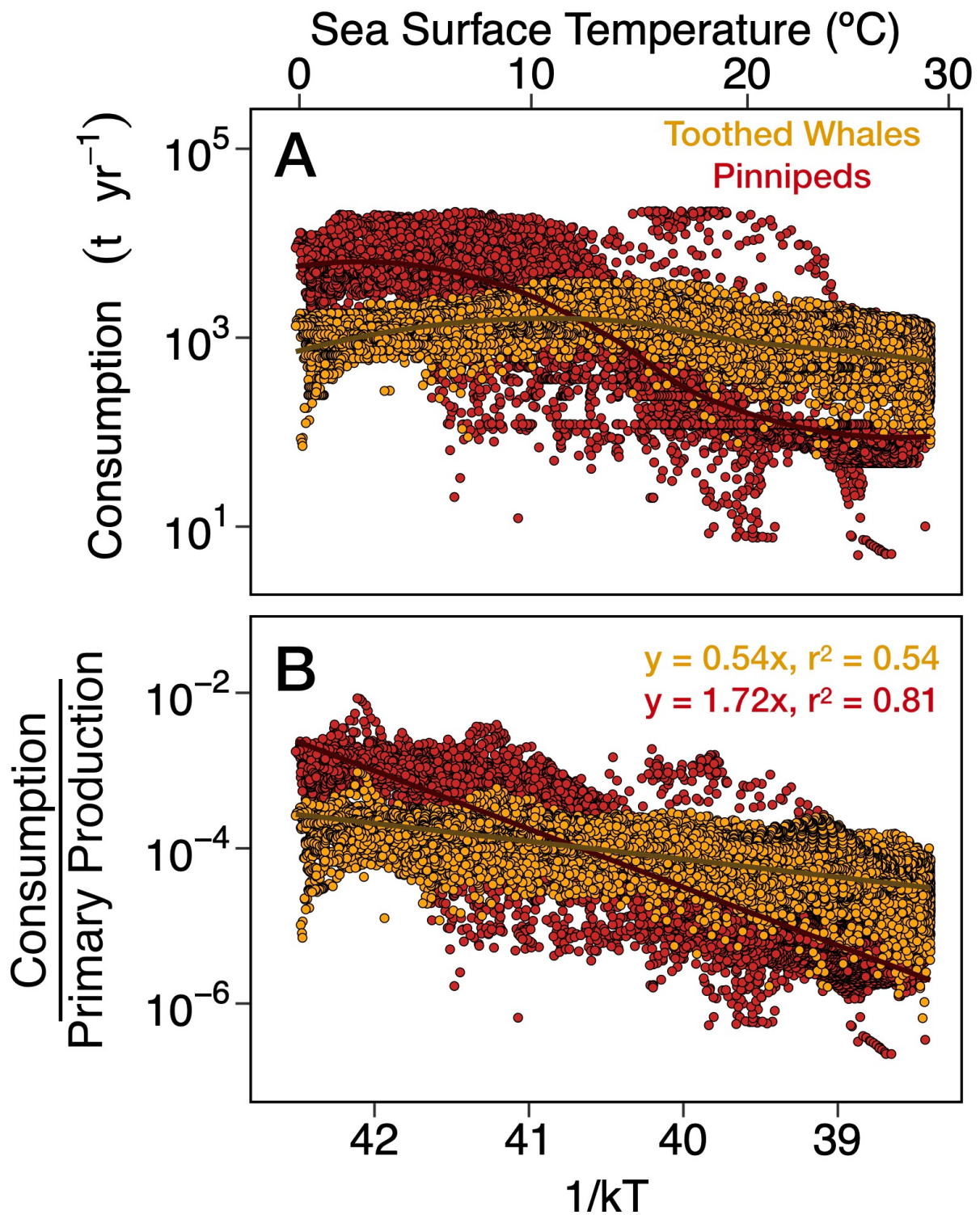
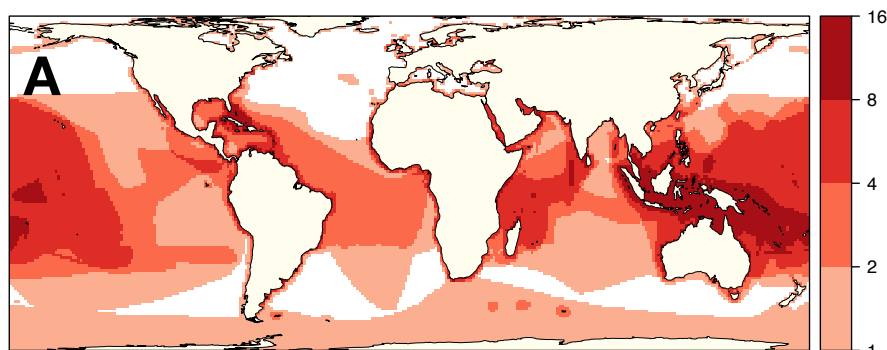


Fig. S9. Pinniped and Odontocete Consumption. For visualization, both sea surface temperature (°C), top, and inverse temperature $1/kT$, bottom are shown. Slopes and fitted lines

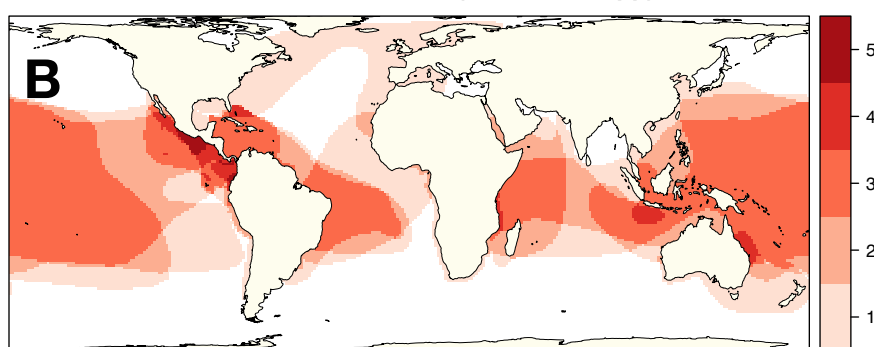
are from regression against $1/kT$, the y axis is logit transformed. Small toothed whales are predominantly delphinids. As slower, solitary foragers compared to delphinids (Fig. 3B), pinnipeds are predicted to be more sensitive to variation in prey speed, and pinniped abundance and collective consumption is expected to decline at greater rates than delphinids in warmer water temperatures. See also Table S1.

Aerial Foraging Birds

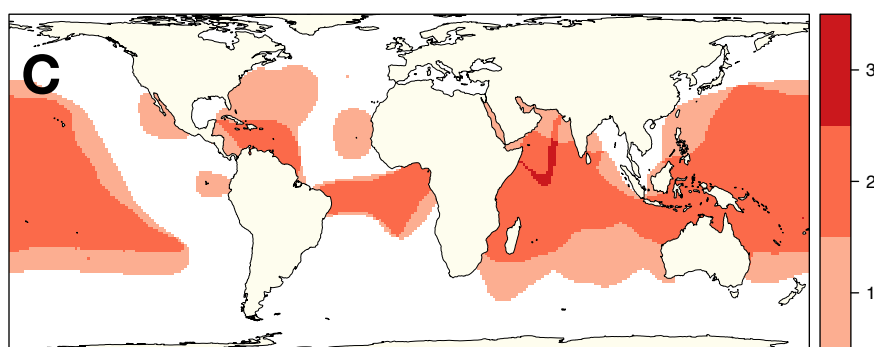
Terns & Noddies (Laridae, 42 spp)



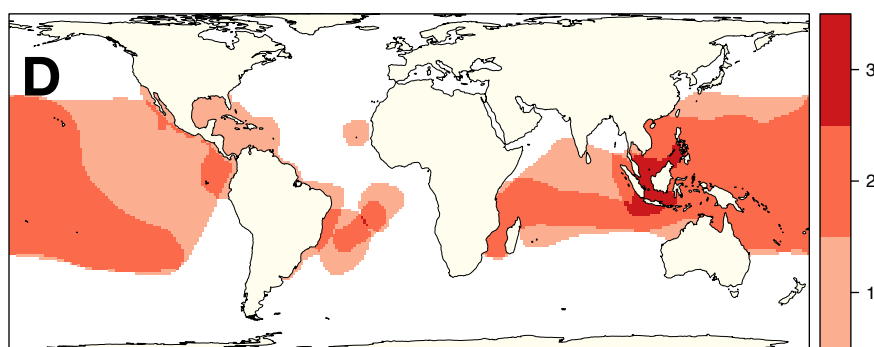
Gannets & Boobies (Sulidae, 10 spp)



Tropicbirds (Phaethontidae, 3 spp)

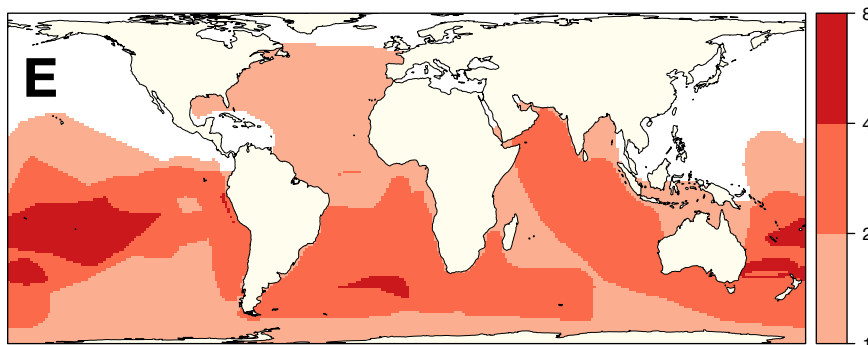


Frigate Birds (Fregatidae, 5 spp)

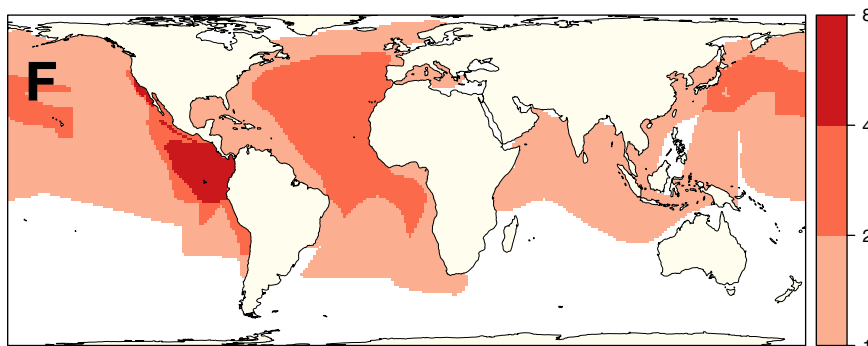


Aerial Foraging Birds

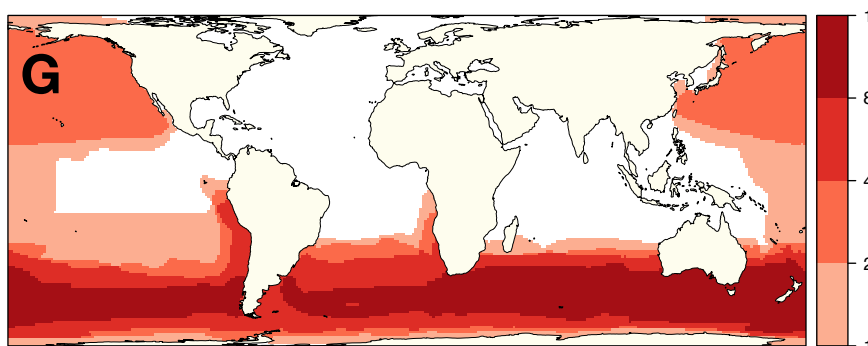
Southern Storm Petrels (Oceanitidae, 9 spp)



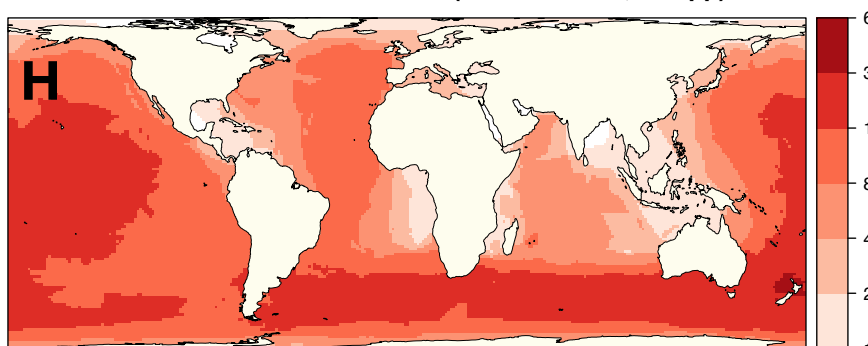
Northern Storm Petrels (Hydrobatidae, 15 spp)



Albatross (Diomedeidae, 22 spp)

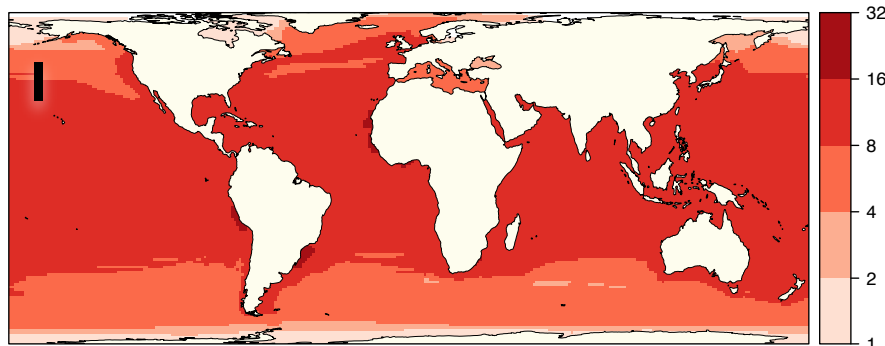


Petrels and Shearwaters (Procellariidae, 96 spp)

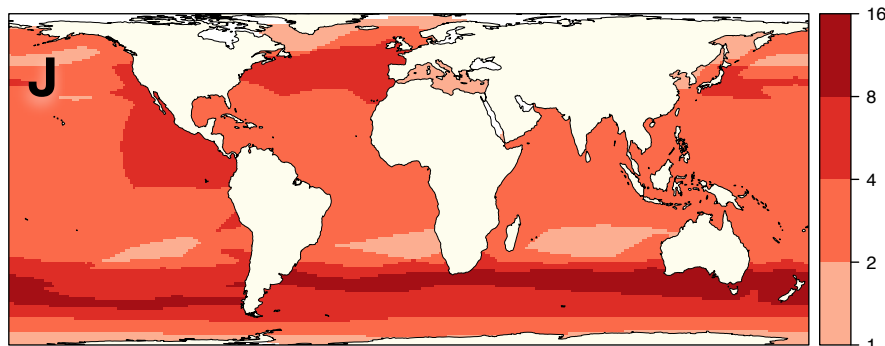


Cooperative & Diving Mammals

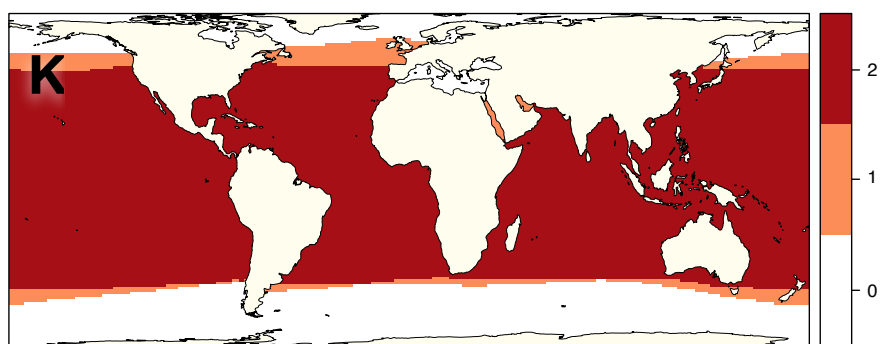
Dolphins (Delphinidae, 68 spp)



Beaked Whales (Ziphiidae, 21 spp)



Dwarf Sperm Whales (Kogiidae, 2 spp)



Sperm Whale (Physeteridae, 1 sp)

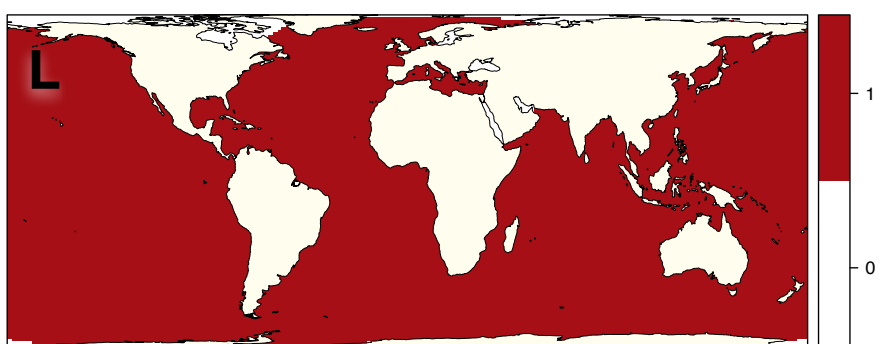


Fig. S10. Exceptions that support the rule: global richness in endotherm families. A-H

Aerial-feeding birds—as opposed to swimming foragers—rely less on active pursuit and have more diverse geographic distributions, including representation in the tropics. **I-L** For marine mammals, cetaceans that cooperate when foraging (**I**) or feed at cold depths (**J-L**) also show variable distributions. In **A**, only marine species of Laridae from the following genera are plotted: *Rissa*, *Sternula*, *Larosterna*, *Sterna*, *Thalasseus*, *Anous*, *Procelsterna*. White cells indicate areas with no recorded species.

Dataset S1. Marine abundance, consumption and relative diversity. Consumption and abundance marine pinniped and small toothed whales (odontocetes excluding sperm and beaked whales) per spatial cell (110 km x 110 km) are provided, as well as richness, environmental data and x, y coordinates in meters. *sstC*: Sea surface temperature ($^{\circ}$ C); *one_kT*: 1/kT (see text); *coastal*: 0 indicates oceanic, 1 indicates coastal; *pinn_abun*: abundance of pinnipeds per cell; *pinn_con*: consumption by pinnipeds ($t \text{ yr}^{-1} \text{ cell}^{-1}$), *ln_endo_ecto_rich*: natural log of endotherm richness to ectotherm richness; *odon_abun*: odontocete abundance per cell; *odon_con*: odontocete consumption ($t \text{ yr}^{-1} \text{ cell}^{-1}$); *OP_abun*: combined odontocete and pinniped abundance per cell; *OP_con*: combined odontocete and pinniped consumption ($t \text{ yr}^{-1} \text{ cell}^{-1}$); *NPP_cb_t_yr*: Net Primary Production from CbPM model (tons wet mass $\text{yr}^{-1} \text{ cell}^{-1}$), *OP_con_NPP_cb*: $OP_{\text{con}} / NPP_{\text{cb}} \text{ t yr}$; *logit_OP_con_NPP_cb*: logit transformed *OP_con_NPP_cb*.

References

1. N. P. Kelley, N. D. Pyenson, Evolutionary innovation and ecology in marine tetrapods from the Triassic to the Anthropocene. *Science* **348**, aaa3716 (2015).
[doi:10.1126/science.aaa3716](https://doi.org/10.1126/science.aaa3716) [Medline](#)
2. J. G. Speight, *Lange's Handbook of Chemistry* (McGraw-Hill, 2005), vol. 1.
3. H. Hillebrand, On the generality of the latitudinal diversity gradient. *Am. Nat.* **163**, 192–211 (2004). [doi:10.1086/381004](https://doi.org/10.1086/381004) [Medline](#)
4. D. K. Cairns, A. J. Gaston, F. Huettmann, Endothermy, ectothermy and the global structure of marine vertebrate communities. *Mar. Ecol. Prog. Ser.* **356**, 239–250 (2008).
[doi:10.3354/meps07286](https://doi.org/10.3354/meps07286)
5. A. I. Dell, S. Pawar, V. M. Savage, Temperature dependence of trophic interactions are driven by asymmetry of species responses and foraging strategy. *J. Anim. Ecol.* **83**, 70–84 (2014). [doi:10.1111/1365-2656.12081](https://doi.org/10.1111/1365-2656.12081) [Medline](#)
6. D. P. Tittensor, C. Mora, W. Jetz, H. K. Lotze, D. Ricard, E. V. Berghe, B. Worm, Global patterns and predictors of marine biodiversity across taxa. *Nature* **466**, 1098–1101 (2010). [doi:10.1038/nature09329](https://doi.org/10.1038/nature09329) [Medline](#)
7. D. P. Faith, Conservation evaluation and phylogenetic diversity. *Biol. Conserv.* **61**, 1–10 (1992). [doi:10.1016/0006-3207\(92\)91201-3](https://doi.org/10.1016/0006-3207(92)91201-3)
8. J. M. Grady, B. J. Enquist, E. Dettweiler-Robinson, N. A. Wright, F. A. Smith, Evidence for mesothermy in dinosaurs. *Science* **344**, 1268–1272 (2014). [doi:10.1126/science.1253143](https://doi.org/10.1126/science.1253143) [Medline](#)
9. D. Bernal, K. A. Dickson, R. E. Shadwick, J. B. Graham, Review: Analysis of the evolutionary convergence for high performance swimming in lamnid sharks and tunas. *Comp. Biochem. Physiol. A* **129**, 695–726 (2001). [doi:10.1016/S1095-6433\(01\)00333-6](https://doi.org/10.1016/S1095-6433(01)00333-6) [Medline](#)
10. A. Berta, J. L. Sumich, K. M. Kovacs, *Marine Mammals: Evolutionary Biology* (Academic Press, 2015).
11. M. L. Brooke, The food consumption of the world's seabirds. *Proc. R. Soc. London Ser. B* **271**, S246–S248 (2004). [doi:10.1098/rsbl.2003.0153](https://doi.org/10.1098/rsbl.2003.0153)
12. K. H. Mann, J. R. Lazier, *Dynamics of Marine Ecosystems: Biological-Physical Interactions in the Oceans* (Wiley, 2013).
13. T. Westberry, M. Behrenfeld, D. Siegel, E. Boss, Carbon-based primary productivity modeling with vertically resolved photoacclimation. *Global Biogeochem. Cycles* **22**, GB2024 (2008). [doi:10.1029/2007GB003078](https://doi.org/10.1029/2007GB003078)

14. C. A. Stock, J. P. Dunne, J. G. John, Global-scale carbon and energy flows through the marine planktonic food web: An analysis with a coupled physical-biological model. *Prog. Oceanogr.* **120**, 1–28 (2014). [doi:10.1016/j.pocean.2013.07.001](https://doi.org/10.1016/j.pocean.2013.07.001)
15. A. P. Allen, J. H. Brown, J. F. Gillooly, Global biodiversity, biochemical kinetics, and the energetic-equivalence rule. *Science* **297**, 1545–1548 (2002).
[doi:10.1126/science.1072380](https://doi.org/10.1126/science.1072380) [Medline](#)
16. D. Tittensor, B. Worm, A neutral-metabolic theory of latitudinal biodiversity. *Glob. Ecol. Biogeogr.* **25**, 630–641 (2016). [doi:10.1111/geb.12451](https://doi.org/10.1111/geb.12451)
17. J. F. Gillooly, J. H. Brown, G. B. West, V. M. Savage, E. L. Charnov, Effects of size and temperature on metabolic rate. *Science* **293**, 2248–2251 (2001).
[doi:10.1126/science.1061967](https://doi.org/10.1126/science.1061967) [Medline](#)
18. A. I. Dell, S. Pawar, V. M. Savage, Systematic variation in the temperature dependence of physiological and ecological traits. *Proc. Natl. Acad. Sci. U.S.A.* **108**, 10591–10596 (2011). [doi:10.1073/pnas.1015178108](https://doi.org/10.1073/pnas.1015178108) [Medline](#)
19. See supplementary materials.
20. S. Pawar, A. I. Dell, V. M. Savage, Dimensionality of consumer search space drives trophic interaction strengths. *Nature* **486**, 485–489 (2012). [doi:10.1038/nature11131](https://doi.org/10.1038/nature11131) [Medline](#)
21. P. Domenici, The scaling of locomotor performance in predator-prey encounters: From fish to killer whales. *Comp. Biochem. Physiol. A* **131**, 169–182 (2001). [doi:10.1016/S1095-6433\(01\)00465-2](https://doi.org/10.1016/S1095-6433(01)00465-2) [Medline](#)
22. K. A. Christian, C. R. Tracy, The effect of the thermal environment on the ability of hatchling Galapagos land iguanas to avoid predation during dispersal. *Oecologia* **49**, 218–223 (1981). [doi:10.1007/BF00349191](https://doi.org/10.1007/BF00349191) [Medline](#)
23. A. Rand, Inverse Relationship Between Temperature and Shyness in the Lizard *Anolis Lineatopus*. *Ecology* **45**, 863–864 (1964). [doi:10.2307/1934935](https://doi.org/10.2307/1934935)
24. R. L. Vaughn, E. Muñiz, J. L. Richardson, B. Würsig, Dolphin Bait-Balling Behaviors in Relation to Prey Ball Escape Behaviors. *Ethology* **117**, 859–871 (2011).
[doi:10.1111/j.1439-0310.2011.01939.x](https://doi.org/10.1111/j.1439-0310.2011.01939.x)
25. K. A. Fritsches, R. W. Brill, E. J. Warrant, Warm eyes provide superior vision in swordfishes. *Curr. Biol.* **15**, 55–58 (2005). [doi:10.1016/j.cub.2004.12.064](https://doi.org/10.1016/j.cub.2004.12.064) [Medline](#)
26. A. M. Magera, J. E. Mills Flemming, K. Kaschner, L. B. Christensen, H. K. Lotze, Recovery trends in marine mammal populations. *PLOS ONE* **8**, e77908 (2013).
[doi:10.1371/journal.pone.0077908](https://doi.org/10.1371/journal.pone.0077908) [Medline](#)
27. K. Kaschner, R. Watson, A. Trites, D. Pauly, Mapping world-wide distributions of marine mammal species using a relative environmental suitability (RES) model. *Mar. Ecol. Prog. Ser.* **316**, 285–310 (2006). [doi:10.3354/meps316285](https://doi.org/10.3354/meps316285)

28. K. Kaschner, thesis, University of British Columbia (2004).
29. D. Pauly, A. Trites, E. Capuli, V. Christensen, Diet composition and trophic levels of marine mammals. *ICES J. Mar. Sci.* **55**, 467–481 (1998). [doi:10.1006/jmsc.1997.0280](https://doi.org/10.1006/jmsc.1997.0280)
30. D. Pauly, V. Christensen, Primary production required to sustain global fisheries. *Nature* **374**, 255–257 (1995). [doi:10.1038/374255a0](https://doi.org/10.1038/374255a0)
31. E. Chassot, S. Bonhommeau, N. K. Dulvy, F. Mélin, R. Watson, D. Gascuel, O. Le Pape, Global marine primary production constrains fisheries catches. *Ecol. Lett.* **13**, 495–505 (2010). [doi:10.1111/j.1461-0248.2010.01443.x](https://doi.org/10.1111/j.1461-0248.2010.01443.x) Medline
32. P. D. van Denderen, M. Lindegren, B. R. MacKenzie, R. A. Watson, K. H. Andersen, Global patterns in marine predatory fish. *Nat. Ecol. Evol.* **2**, 65–70 (2018). [doi:10.1038/s41559-017-0388-z](https://doi.org/10.1038/s41559-017-0388-z)
33. T. Roslin, B. Hardwick, V. Novotny, W. K. Petry, N. R. Andrew, A. Asmus, I. C. Barrio, Y. Bassett, A. L. Boesing, T. C. Bonebrake, E. K. Cameron, W. Dátilo, D. A. Donoso, P. Drozd, C. L. Gray, D. S. Hik, S. J. Hill, T. Hopkins, S. Huang, B. Koane, B. Laird-Hopkins, L. Laukkonen, O. T. Lewis, S. Milne, I. Mwesige, A. Nakamura, C. S. Nell, E. Nichols, A. Prokurat, K. Sam, N. M. Schmidt, A. Slade, V. Slade, A. Suchanková, T. Teder, S. van Nouhuys, V. Vandvik, A. Weissflog, V. Zhukovich, E. M. Slade, Higher predation risk for insect prey at low latitudes and elevations. *Science* **356**, 742–744 (2017). [doi:10.1126/science.aaj1631](https://doi.org/10.1126/science.aaj1631) Medline
34. D. Wright, Species-Energy Theory: An Extension of Species-Area Theory. *Oikos* **41**, 496–506 (1983). [doi:10.2307/3544109](https://doi.org/10.2307/3544109)
35. A. E. Moura, J. G. Kenny, R. R. Chaudhuri, M. A. Hughes, R. R. Reisinger, P. J. N. de Bruyn, M. E. Dahlheim, N. Hall, A. R. Hoelzel, Phylogenomics of the killer whale indicates ecotype divergence in sympatry. *Heredity* **114**, 48–55 (2015). [doi:10.1038/hdy.2014.67](https://doi.org/10.1038/hdy.2014.67) Medline
36. K. J. Gaston, T. M. Blackburn, J. H. Lawton, Interspecific Abundance-Range Size Relationships: An Appraisal of Mechanisms. *J. Anim. Ecol.* **66**, 579–601 (1997). [doi:10.2307/5951](https://doi.org/10.2307/5951)
37. M. P. Hare, F. Cipriano, S. R. Palumbi, Genetic evidence on the demography of speciation in allopatric dolphin species. *Evolution* **56**, 804–816 (2002). [doi:10.1111/j.0014-3820.2002.tb01391.x](https://doi.org/10.1111/j.0014-3820.2002.tb01391.x) Medline
38. K. Longenecker, Fishes in the Hawaiian monk seal diet, based on regurgitate samples collected in the Northwestern Hawaiian Islands. *Mar. Mamm. Sci.* **26**, 420–429 (2010). [doi:10.1111/j.1748-7692.2009.00332.x](https://doi.org/10.1111/j.1748-7692.2009.00332.x)
39. T. Sasaki, M. Nikaido, S. Wada, T. K. Yamada, Y. Cao, M. Hasegawa, N. Okada, Balaenoptera omurai is a newly discovered baleen whale that represents an ancient

evolutionary lineage. *Mol. Phylogenet. Evol.* **41**, 40–52 (2006).
[doi:10.1016/j.ympev.2006.03.032](https://doi.org/10.1016/j.ympev.2006.03.032) [Medline](#)

40. D. Lee, P. Reddish, Plummeting gannets: A paradigm of ecological optics. *Nature* **293**, 293–294 (1981). [doi:10.1038/293293a0](https://doi.org/10.1038/293293a0)
41. C. Duffy, G. Taylor, *Bull. Auckland Mus.* **20**, 497–500 (2015).
42. P. Bertilsson-Friedman, Distribution and frequencies of shark-inflicted injuries to the endangered Hawaiian monk seal (*Monachus schauinslandi*). *J. Zool.* **268**, 361–368 (2006). [doi:10.1111/j.1469-7998.2006.00066.x](https://doi.org/10.1111/j.1469-7998.2006.00066.x)
43. R. A. Martin, N. Hammerschlag, R. S. Collier, C. Fallows, Predatory behaviour of white sharks (*Carcharodon carcharias*) at Seal Island, South Africa. *J. Mar. Biol. Assoc. U.K.* **85**, 1121–1136 (2005). [doi:10.1017/S002531540501218X](https://doi.org/10.1017/S002531540501218X)
44. C. Lydersen, A. T. Fisk, K. M. Kovacs, A review of Greenland shark (*Somniosus microcephalus*) studies in the Kongsfjorden area, Svalbard Norway. *Polar Biol.* **39**, 2169–2178 (2016). [doi:10.1007/s00300-016-1949-3](https://doi.org/10.1007/s00300-016-1949-3)
45. B. A. Block, H. Dewar, S. B. Blackwell, T. D. Williams, E. D. Prince, C. J. Farwell, A. Boustany, S. L. Teo, A. Seitz, A. Walli, D. Fudge, Migratory movements, depth preferences, and thermal biology of Atlantic bluefin tuna. *Science* **293**, 1310–1314 (2001). [doi:10.1126/science.1061197](https://doi.org/10.1126/science.1061197) [Medline](#)
46. D. W. Sims, V. J. Wearmouth, E. J. Southall, J. M. Hill, P. Moore, K. Rawlinson, N. Hutchinson, G. C. Budd, D. Righton, J. D. Metcalfe, J. P. Nash, D. Morritt, Hunt warm, rest cool: Bioenergetic strategy underlying diel vertical migration of a benthic shark. *J. Anim. Ecol.* **75**, 176–190 (2006). [doi:10.1111/j.1365-2656.2005.01033.x](https://doi.org/10.1111/j.1365-2656.2005.01033.x) [Medline](#)
47. T. Kitagawa, S. Kimura, H. Nakata, H. Yamada, Thermal adaptation of Pacific bluefin tuna *Thunnus orientalis* to temperate waters. *Fish. Sci.* **72**, 149–156 (2006). [doi:10.1111/j.1444-2906.2006.01129.x](https://doi.org/10.1111/j.1444-2906.2006.01129.x)
48. B. Bogstad, H. Gjøsæter, T. Haug, U. Lindstrøm, *Front. Ecol. Evol.* **3**, 29 (2015). [doi:10.3389/fevo.2015.00029](https://doi.org/10.3389/fevo.2015.00029)
49. J. P. Croxall, P. N. Trathan, E. J. Murphy, Environmental change and Antarctic seabird populations. *Science* **297**, 1510–1514 (2002). [doi:10.1126/science.1071987](https://doi.org/10.1126/science.1071987) [Medline](#)
50. J. P. Gattuso, A. Magnan, R. Billé, W. W. L. Cheung, E. L. Howes, F. Joos, D. Allemand, L. Bopp, S. R. Cooley, C. M. Eakin, O. Hoegh-Guldberg, R. P. Kelly, H.-O. Pörtner, A. D. Rogers, J. M. Baxter, D. Laffoley, D. Osborn, A. Rankovic, J. Rochette, U. R. Sumaila, S. Treyer, C. Turley, Contrasting futures for ocean and society from different anthropogenic CO₂ emissions scenarios. *Science* **349**, aac4722 (2015). [doi:10.1126/science.aac4722](https://doi.org/10.1126/science.aac4722) [Medline](#)

51. BirdLife International and NatureServe, *Bird Species Distribution Maps of the World* (BirdLife International and Handbook of the Birds of the World, 2017);
<http://datazone.birdlife.org/species/requestdis>.
52. IUCN, *IUCN Red List of Threatened Species* Version 5.2 (2017); www.iucnredlist.org.
53. K. Kaschner, K. Kesner-Reyes, C. Garilao, J. Rius-Barile, T. Rees, R. Froese, AquaMaps: Predicted Range Maps for Aquatic Species (2016); www.aquamaps.org.
54. R: A Language and Environment for Statistical Computing (R Foundation for Statistical Computing, Vienna, 2012).
55. S. Faurby, J.-C. Svenning, A species-level phylogeny of all extant and late Quaternary extinct mammals using a novel heuristic-hierarchical Bayesian approach. *Mol. Phylogenet. Evol.* **84**, 14–26 (2015). [doi:10.1016/j.ympev.2014.11.001](https://doi.org/10.1016/j.ympev.2014.11.001) [Medline](#)
56. R. A. Pyron, F. T. Burbrink, J. J. Wiens, A phylogeny and revised classification of Squamata, including 4161 species of lizards and snakes. *BMC Evol. Biol.* **13**, 93 (2013). [doi:10.1186/1471-2148-13-93](https://doi.org/10.1186/1471-2148-13-93) [Medline](#)
57. L. Sorenson, F. Santini, M. E. Alfaro, The effect of habitat on modern shark diversification. *J. Evol. Biol.* **27**, 1536–1548 (2014). [doi:10.1111/jeb.12405](https://doi.org/10.1111/jeb.12405) [Medline](#)
58. D. L. Rabosky, F. Santini, J. Eastman, S. A. Smith, B. Sidlauskas, J. Chang, M. E. Alfaro, Rates of speciation and morphological evolution are correlated across the largest vertebrate radiation. *Nat. Commun.* **4**, 1958 (2013). [doi:10.1038/ncomms2958](https://doi.org/10.1038/ncomms2958) [Medline](#)
59. W. Jetz, G. H. Thomas, J. B. Joy, K. Hartmann, A. O. Mooers, The global diversity of birds in space and time. *Nature* **491**, 444–448 (2012). [doi:10.1038/nature11631](https://doi.org/10.1038/nature11631) [Medline](#)
60. S. W. Kembel, P. D. Cowan, M. R. Helmus, W. K. Cornwell, H. Morlon, D. D. Ackerly, S. P. Blomberg, C. O. Webb, Picante: R tools for integrating phylogenies and ecology. *Bioinformatics* **26**, 1463–1464 (2010). [doi:10.1093/bioinformatics/btq166](https://doi.org/10.1093/bioinformatics/btq166) [Medline](#)
61. J. Besag, J. York, A. Mollié, Bayesian image restoration, with two applications in spatial statistics. *Ann. Inst. Stat. Math.* **43**, 1–20 (1991). [doi:10.1007/BF00116466](https://doi.org/10.1007/BF00116466)
62. F. Lindgren, H. Rue, Bayesian spatial modelling with R-INLA. *J. Stat. Softw.* 10.18637/jss.v063.i19 (2015). [doi:10.18637/jss.v063.i19](https://doi.org/10.18637/jss.v063.i19)
63. R. Bivand, V. Gómez-Rubio, H. Rue, Spatial data analysis with R-INLA with some extensions. *J. Stat. Softw.* 10.18637/jss.v063.i20 (2015). [doi:10.18637/jss.v063.i20](https://doi.org/10.18637/jss.v063.i20)
64. J. del Hoyo, A. Elliot, J. Sargatal, D. A. Christie, E. de Juana, in *Handbook of Birds of the World Alive* (Lynx, Barcelona, 2016).
65. S. L. Gallon, C. E. Sparling, J.-Y. Georges, M. A. Fedak, M. Biuw, D. Thompson, How fast does a seal swim? Variations in swimming behaviour under differing foraging conditions. *J. Exp. Biol.* **210**, 3285–3294 (2007). [doi:10.1242/jeb.007542](https://doi.org/10.1242/jeb.007542) [Medline](#)

66. S. D. Feldkamp, Swimming in the California sea lion: Morphometrics, drag and energetics. *J. Exp. Biol.* **131**, 117–135 (1987). [Medline](#)
67. O. Cheneval, R. Blake, A. Trites, K. Chan, Turning maneuvers in Steller sea lions (*Eumatopias jubatus*). *Mar. Mamm. Sci.* **23**, 94–109 (2007). [doi:10.1111/j.1748-7692.2006.00094.x](https://doi.org/10.1111/j.1748-7692.2006.00094.x)
68. P. J. Ponganis, E. P. Ponganis, K. V. Ponganis, G. L. Kooyman, R. L. Gentry, F. Trillmich, Swimming velocities in otariids. *Can. J. Zool.* **68**, 2105–2112 (1990). [doi:10.1139/z90-293](https://doi.org/10.1139/z90-293)
69. I. Boyd, K. Reid, R. Bevan, Swimming speed and allocation of time during the dive cycle in Antarctic fur seals. *Anim. Behav.* **50**, 769–784 (1995). [doi:10.1016/0003-3472\(95\)80137-5](https://doi.org/10.1016/0003-3472(95)80137-5)
70. D. Crocker, N. Gales, D. Costa, Swimming speed and foraging strategies of New Zealand sea lions (*Phocarctos hookeri*). *J. Zool.* **254**, 267–277 (2001).
[doi:10.1017/S0952836901000784](https://doi.org/10.1017/S0952836901000784)
71. Y. Ropert-Coudert, K. Sato, A. Kato, J.-B. Charrassin, C. A. Bost, Y. Le Maho, Y. Naito, Preliminary investigations of prey pursuit and capture by king penguins at sea. *Polar Biosci.* **13**, 101–112 (2000).
72. G. L. Kooyman, P. J. Ponganis, M. A. Castellini, E. P. Ponganis, K. V. Ponganis, P. H. Thorson, S. A. Eckert, Y. LeMaho, Heart rates and swim speeds of emperor penguins diving under sea ice. *J. Exp. Biol.* **165**, 161–180 (1992). [Medline](#)
73. B. Culik, R. P. Wilson, Swimming energetics and performance of instrumented Adélie penguins (*Pygoscelis adeliae*). *J. Exp. Biol.* **158**, 355–368 (1991).
74. R. P. Wilson, Y. Ropert-Coudert, A. Kato, Rush and grab strategies in foraging marine endotherms: The case for haste in penguins. *Anim. Behav.* **63**, 85–95 (2002).
[doi:10.1006/anbe.2001.1883](https://doi.org/10.1006/anbe.2001.1883)
75. F. E. Fish, C. A. Hui, Dolphin swimming—a review. *Mammal Rev.* **21**, 181–195 (1991).
[doi:10.1111/j.1365-2907.1991.tb00292.x](https://doi.org/10.1111/j.1365-2907.1991.tb00292.x)
76. J. Rohr, F. Fish, J. Gilpatrick, Maximum swim speeds of captive and free-ranging delphinids: Critical analysis of extraordinary performance. *Mar. Mamm. Sci.* **18**, 1–19 (2002).
[doi:10.1111/j.1748-7692.2002.tb01014.x](https://doi.org/10.1111/j.1748-7692.2002.tb01014.x)
77. J. Videler, C. Wardle, Fish swimming stride by stride: Speed limits and endurance. *Rev. Fish Biol. Fish.* **1**, 23–40 (1991). [doi:10.1007/BF00042660](https://doi.org/10.1007/BF00042660)
78. C. Wardle, in *Environmental Physiology of Fishes*, M. Ali, Ed. (Springer, 1980), pp. 519–531.

79. T. Kubo, W. Sakamoto, O. Murata, H. Kumai, Whole-body heat transfer coefficient and body temperature change of juvenile Pacific bluefin tuna *Thunnus orientalis* according to growth. *Fish. Sci.* **74**, 995–1004 (2008). [doi:10.1111/j.1442-2906.2008.01617.x](https://doi.org/10.1111/j.1442-2906.2008.01617.x)
80. N. K. Dulvy, Y. Sadovy, J. D. Reynolds, Extinction vulnerability in marine populations. *Fish Fish.* **4**, 25–64 (2003). [doi:10.1046/j.1467-2979.2003.00105.x](https://doi.org/10.1046/j.1467-2979.2003.00105.x)
81. B. A. Block, I. D. Jonsen, S. J. Jorgensen, A. J. Winship, S. A. Shaffer, S. J. Bograd, E. L. Hazen, D. G. Foley, G. A. Breed, A.-L. Harrison, J. E. Ganong, A. Swithenbank, M. Castleton, H. Dewar, B. R. Mate, G. L. Shillinger, K. M. Schaefer, S. R. Benson, M. J. Weise, R. W. Henry, D. P. Costa, Tracking apex marine predator movements in a dynamic ocean. *Nature* **475**, 86–90 (2011). [doi:10.1038/nature10082](https://doi.org/10.1038/nature10082) [Medline](#)
82. R. C. Rocha Jr., P. J. Clapham, Y. V. Ivashchenko, Emptying the oceans: A summary of industrial whaling catches in the 20th century. *Mar. Fish. Rev.* **76**, 37–48 (2014). [doi:10.7755/MFR.76.4.3](https://doi.org/10.7755/MFR.76.4.3)
83. C. Barnes, D. Maxwell, D. C. Reuman, S. Jennings, Global patterns in predator-prey size relationships reveal size dependency of trophic transfer efficiency. *Ecology* **91**, 222–232 (2010). [doi:10.1890/08-2061.1](https://doi.org/10.1890/08-2061.1) [Medline](#)
84. R. Froese, D. Pauly, Fishbase (2017); www.fishbase.org.
85. X. Irigoien, T. A. Klevjer, A. Røstad, U. Martinez, G. Boyra, J. L. Acuña, A. Bode, F. Echevarria, J. I. Gonzalez-Gordillo, S. Hernandez-Leon, S. Agusti, D. L. Aksnes, C. M. Duarte, S. Kaartvedt, Large mesopelagic fishes biomass and trophic efficiency in the open ocean. *Nat. Commun.* **5**, 3271 (2014). [doi:10.1038/ncomms4271](https://doi.org/10.1038/ncomms4271) [Medline](#)
86. W. R. Burnside, E. B. Erhardt, S. T. Hammond, J. H. Brown, Rates of biotic interactions scale predictably with temperature despite variation. *Oikos* **123**, 1449–1456 (2014). [doi:10.1111/oik.01199](https://doi.org/10.1111/oik.01199)
87. C. S. Holling, Some characteristics of simple types of predation and parasitism. *Can. Entomol.* **91**, 385–398 (1959). [doi:10.4039/Ent91385-7](https://doi.org/10.4039/Ent91385-7)
88. P. Weatherall, K. M. Marks, M. Jakobsson, T. Schmitt, S. Tani, J. E. Arndt, M. Rovere, D. Chayes, V. Ferrini, R. Wigley, A new digital bathymetric model of the world's oceans. *Earth Space Sci.* **2**, 331–345 (2015). [doi:10.1002/2015EA000107](https://doi.org/10.1002/2015EA000107)
89. GEBCO One Minute Grid. Version 2008–2002 (2015); www.bodc.ac.uk/data/hosted_data_systems/gebco_gridded_bathymetry_data/.
90. http://iridl.ldeo.columbia.edu/SOURCES/.NOAA/.NCEP/.EMC/.CMB/.GLOBAL/.Reyn_SmithOIv2/.monthly/.sea_ice/.

91. R. W. Reynolds, N. A. Rayner, T. M. Smith, D. C. Stokes, W. Wang, An improved in situ and satellite SST analysis for climate. *J. Clim.* **15**, 1609–1625 (2002). [doi:10.1175/1520-0442\(2002\)015<1609:AIISAS>2.0.CO;2](https://doi.org/10.1175/1520-0442(2002)015<1609:AIISAS>2.0.CO;2)
92.
http://iridl.ldeo.columbia.edu/SOURCES/.NOAA/.NCEP/.EMC/.CMB/.GLOBAL/.Reyn_SmithOIv2/.monthly/.dataset_documentation.html.
93. M. J. Behrenfeld, P. G. Falkowski, Photosynthetic rates derived from satellite-based chlorophyll concentration. *Limnol. Oceanogr.* **42**, 1–20 (1997).
[doi:10.4319/lo.1997.42.1.0001](https://doi.org/10.4319/lo.1997.42.1.0001)
94. www.science.oregonstate.edu/ocean/productivity/index.php.
95. P. Assmy, J. K. Ehn, M. Fernández-Méndez, H. Hop, C. Katlein, A. Sundfjord, K. Bluhm, M. Daase, A. Engel, A. Fransson, M. A. Granskog, S. R. Hudson, S. Kristiansen, M. Nicolaus, I. Peeken, A. H. H. Renner, G. Spreen, A. Tatarek, J. Wiktor, Floating ice-algal aggregates below melting arctic sea ice. *PLOS ONE* **8**, e76599 (2013).
[doi:10.1371/journal.pone.0076599](https://doi.org/10.1371/journal.pone.0076599) [Medline](#)
96. R. W. Eppley, Temperature and phytoplankton growth in the sea. *Fish Bull.* **70**, 1063–1085 (1972).
97. A. Morel, Light and marine photosynthesis: A spectral model with geochemical and climatological implications. *Prog. Oceanogr.* **26**, 263–306 (1991). [doi:10.1016/0079-6611\(91\)90004-6](https://doi.org/10.1016/0079-6611(91)90004-6)
98. M. J. Behrenfeld, E. Boss, D. A. Siegel, D. M. Shea, Carbon-based ocean productivity and phytoplankton physiology from space. *Global Biogeochem. Cycles* **19**, GB1006 (2005).
[doi:10.1029/2004GB002299](https://doi.org/10.1029/2004GB002299)
99. J. C. Goldman, E. J. Carpenter, A kinetic approach to the effect of temperature on algal growth. *Limnol. Oceanogr.* **19**, 756–766 (1974). [doi:10.4319/lo.1974.19.5.0756](https://doi.org/10.4319/lo.1974.19.5.0756)
100. J. E. Bissinger, D. J. Montagnes, J. Sharples, D. Atkinson, Predicting marine phytoplankton maximum growth rates from temperature: Improving on the Eppley curve using quantile regression. *Limnol. Oceanogr.* **53**, 487–493 (2008). [doi:10.4319/lo.2008.53.2.0487](https://doi.org/10.4319/lo.2008.53.2.0487)
101. V. Saba, M. A. M. Friedrichs, D. Antoine, R. A. Armstrong, I. Asanuma, M. J. Behrenfeld, A. M. Ciotti, M. Dowell, N. Hoepffner, K. J. W. Hyde, J. Ishizaka, T. Kameda, J. Marra, F. Mélin, A. Morel, J. O'Reilly, M. Scardi, W. O. Smith Jr., T. J. Smyth, S. Tang, J. Uitz, K. Waters, T. K. Westberry, An evaluation of ocean color model estimates of marine primary productivity in coastal and pelagic regions across the globe. *Biogeosciences* **8**, 489–503 (2011). [doi:10.5194/bg-8-489-2011](https://doi.org/10.5194/bg-8-489-2011)

102. M. J. Behrenfeld, E. S. Boss, Resurrecting the ecological underpinnings of ocean plankton blooms. *Annu. Rev. Mar. Sci.* **6**, 167–194 (2014). [doi:10.1146/annurev-marine-052913-021325](https://doi.org/10.1146/annurev-marine-052913-021325) [Medline](#)
103. P. G. Falkowski, C. N. Flagg, G. T. Rowe, S. L. Smith, T. E. Whitledge, C. D. Wirick, The fate of a spring phytoplankton bloom: Export or oxidation? *Cont. Shelf Res.* **8**, 457–484 (1988). [doi:10.1016/0278-4343\(88\)90064-7](https://doi.org/10.1016/0278-4343(88)90064-7)
104. C. Stock, J. Dunne, J. John, Drivers of trophic amplification of ocean productivity trends in a changing climate. *Biogeosciences* **11**, 7125–7135 (2014). [doi:10.5194/bg-11-7125-2014](https://doi.org/10.5194/bg-11-7125-2014)
105. J. H. Ryther, Photosynthesis and fish production in the sea. *Science* **166**, 72–76 (1969). [doi:10.1126/science.166.3901.72](https://doi.org/10.1126/science.166.3901.72) [Medline](#)
106. E. San Martin, X. Irigoien, H. Roger P, Á. L. Urrutia, M. V. Zubkov, J. L. Heywood, Variation in the transfer of energy in marine plankton along a productivity gradient in the Atlantic Ocean. *Limnol. Oceanogr.* **51**, 2084–2091 (2006). [doi:10.4319/lo.2006.51.5.2084](https://doi.org/10.4319/lo.2006.51.5.2084)
107. P. Domenici, R. Blake, The kinematics and performance of fish fast-start swimming. *J. Exp. Biol.* **200**, 1165–1178 (1997). [Medline](#)
108. M. A. Peck, L. J. Buckley, D. A. Bengtson, Effects of temperature and body size on the swimming speed of larval and juvenile Atlantic cod (*Gadus morhua*): Implications for individual-based modelling. *Environ. Biol. Fishes* **75**, 419–429 (2006). [doi:10.1007/s10641-006-0031-3](https://doi.org/10.1007/s10641-006-0031-3)
109. J. C. Montgomery, A. R. McVean, D. McCarthy, The effects of lowered temperature on spontaneous eye movements in a teleost fish. *Comp. Biochem. Physiol. A* **75**, 363–368 (1983). [doi:10.1016/0300-9629\(83\)90094-4](https://doi.org/10.1016/0300-9629(83)90094-4) [Medline](#)
110. M. Friedlander, N. Kotchabhakdi, C. Prosser, Effects of cold and heat on behavior and cerebellar function in goldfish. *J. Comp. Physiol.* **112**, 19–45 (1976). [doi:10.1007/BF00612674](https://doi.org/10.1007/BF00612674)